

# **Development of pressure sensors based on printed electronics for application in robotics**

**Rui Daniel Ribeiro Dias**

Thesis to obtain the Master of Science Degree in

## **Bioengineering and Nanosystems**

Supervisor: Prof.Dr Jorge Manuel Ferreira Morgado  
Supervisor: Eng. Joana Almeida

### **Examination Committee**

Chairperson: Prof.Dr Gabriel Antonio Amaro Monteiro  
Supervisor: Prof.Dr Jorge Manuel Ferreira Morgado  
Members of the Committee: Prof.Dr Frederico Castelo Alves Ferreira

**October 2020**

## **Preface**

The work presented in this thesis was performed at Instituto de Telecomunicações(organic electronics group) at Instituto Superior Técnico (Lisboa, Portugal), during the period February- October 2019, under the supervision of Prof.Dr Jorge Morgado, in collaboration with Center of Nanotechnologies and Smart Materials(CeNTI), under the supervision of Eng. Joana Almeida.

## **Declaration**

I declare that this document is an original work of my own authorship and that it fulfills all the requirements of the Code of Conduct and Good Practices of the Universidade de Lisboa.

## 0.1 Acknowledgements

I would like to start by thanking my supervisor Prof. Jorge Morgado for all help, orientation and knowledge shared during his classes and along this project. Would like to thank Eng. Joana Almeida and Eng. Agnieszka Jóskowiak at CeNTI for all help given on this project. Ana Barros and Eduardo Oliveira for their assistance during the preparation of PDMS/Carbon nanotubes nanocomposites and respective DMA analysis. A special thanks to my mom, dad and brother for all the patience, love and motivational talks during this amazing journey at Instituto Superior Técnico. Not all this had been possible without the unbelievable help of my precious family in Lisbon. This being said, a special thank to my godmother Tânia, Hugo and my aunt Alice who offered me a place to stay and always helped me in everything . To my dear friends Prata, Manuel, Pedro, Rafael, Inês and Joana an amazing thank you for all the good moments, dinners, parties and holidays we shared together. I hope our friendship will last forever.

Last but not least, an enormous thank you to my beautiful wife Sthefanie Costa for all help, patience and love shared during our lives together but specially during the realization of this project.

## 0.2 Resumo

Desde os primórdios da humanidade que se verifica uma constante evolução dos materiais, processos e tecnologias utilizadas. Esta evolução teve um tremendo impacto na vida das pessoas. Hoje em dia a tecnologia existente permite fazer certas actividades que há 10 anos atrás seriam impensáveis. Com o progresso da tecnologia e o conhecimento sobre o que nos rodeia, tornou muito mais fácil a investigação científica e o desenvolvimento de novos materiais. Com isto, e pensando na era em que se vive, o desenvolvimento de materiais que possuem características eléctricas, mas que são flexíveis e moldáveis aumentou uma vez que podem ser aplicados em diversas áreas, desde equipamentos médicos até usos mais comuns como telemóveis dobráveis. Neste estudo foram caracterizados mecânica, térmica e electricamente várias amostras do nanocompositos polidimetilsiloxano/nanotubos de carbono de parede múltipla (PDMS/MWCNT) com diferentes concentrações de nanotubos e densidade de ligações cruzadas.

Verificou-se , no geral, o aumento do módulo com o aumento da percentagem de nanotubos de carbono(NC), em ensaios DMA. Nos ensaios eléctricos verificou-se que o aumento da percentagem de NC aumenta a condutividade eléctrica do compósito e que esta diminui com o aumento da temperatura. O impacto nas propriedades eléctricas dos ensaios DMA também foi analisado, não se tendo obtido nenhuma conclusão dada a dispersão dos resultados.

### 0.3 Abstract

Since the dawn of humanity, there has been a constant evolution of the materials, processes and technologies used. This evolution has had a tremendous impact on people's lives. The technology of today allows us to do certain activities that years ago would have been unthinkable. With the progress of technology and the knowledge about what surrounds us, the development of new materials became more possible. With this in mind, it was expected the development of new materials(composites) that combine characteristics of very different materials. Materials that are flexible and electric conductors are in high demand, not only for commons uses( flexible screens, wearable phones) but also for other areas such as medicine and bio engineering. In this study, 12 polydimethylsiloxane / multi-walled carbon nanotubes (PDMS / MWCNT) with different concentrations of nanotubes and cross-link density. were characterized mechanically, thermally and electrically.

In general, it was observed an increase of the modulus with the increase of percentage of carbon nanotubes (CN) in DMA tests. In electrical tests, it was found that higher percentage of CN leads to a more electrical conductive material. Variation of electrical resistance with temperature was assessed and it was verified that the resistance increases. The impact of DMA tests on the electrical properties of PDMS/MWCNT was also analyzed, but no conclusion could be obtained.

# Contents

0.1	Acknowledgements . . . . .	3
0.2	Resumo . . . . .	4
0.3	Abstract . . . . .	5
<b>1</b>	<b>Introduction</b>	<b>8</b>
1.1	Motivation . . . . .	8
1.2	Pressure sensor . . . . .	9
1.3	Polymers and polymer nanocomposites . . . . .	10
1.4	Carbon allotropes . . . . .	12
1.5	Carbon nanotubes . . . . .	14
1.6	PDMS . . . . .	16
1.7	Polymer/carbon nanotubes nanocomposites . . . . .	18
1.7.1	PDMS/carbon nanotube preparation . . . . .	21
1.8	Techniques . . . . .	22
1.8.1	Electrical Characterization . . . . .	22
1.8.2	Mechanical Properties . . . . .	24
1.9	Research Objectives . . . . .	27
1.10	Research Strategy . . . . .	27
<b>2</b>	<b>PDMS/carbon nanotube preparation protocol</b>	<b>28</b>
2.1	Materials . . . . .	28
2.2	Samples Preparation and Characterization . . . . .	28
<b>3</b>	<b>Results</b>	<b>29</b>
3.1	Dynamic Mechanical Analysis of PDMS/MWCNT nanocomposite . . . . .	30
3.2	Electrical properties of PDMS/carbon nanotubes composites . . . . .	38
3.2.1	Electrical characterization . . . . .	38
3.2.2	Effect of temperature on the electrical resistance . . . . .	40
3.2.3	Influence of the DMA studies on the electrical properties . . . . .	42
3.2.4	Sensing effect of applied stress on materials resistance . . . . .	43
<b>4</b>	<b>Conclusions</b>	<b>44</b>
<b>5</b>	<b>Institutes</b>	<b>45</b>

## List of Figures

1	Simplified scheme of a Sensor . . . . .	9
2	The Maxwell model . . . . .	10
3	Stress relaxation . . . . .	11
4	Schematic variation of the E/elastic modulus of a polymer with temperature. . . . .	11
5	Diamond and graphite structure . . . . .	12
6	Buckminsterfullerene C <sub>60</sub> . . . . .	13
7	Single walled carbon nanotube . . . . .	13
8	Multi walled carbon nanotube . . . . .	15
9	PDMS chemical structure . . . . .	16
10	PDMS Sylgard 184 . . . . .	16
11	Elastic modulus for samples prepared at different curing temperatures [1] . . . . .	17
12	Resistance Vs Force [2] . . . . .	18
13	Resistance response with cyclic strain for a 4% MWCNT containing PDMS/MEP/MWCNT composite [3] . . . . .	19
14	Percolation threshold[4] . . . . .	19
15	Conductive network formation[4] . . . . .	19
16	Distribution of micro- and nano-scale fillers of the same 0.1 vol.% in a reference volume of 1 mm <sup>3</sup> (A: Al <sub>2</sub> O <sub>3</sub> particle; B: carbon fiber; C: GNP; D: CN). [5] . . . . .	20
17	Four Point Probe Method . . . . .	22
18	Transitions in amorphous polymers as detected by the loss tangent (Reproduced from “Acoustic Methods of Investigating Polymers”, I. Perepechko (translated by G. Leib), Mir Publishers, Moscow, 1975) . . . . .	25
19	Comparison of the loss peaks in semicrystalline and amorphous polymers. Reproduced from “Thermal Analysis of Polymers-Fundamentals and applications”, Joseph D. Menczel and R. Bruce Prime, eds, Wiley, 2009 . . . . .	26
20	Variation of storage modulus (E’), loss modulus (E’’) and loss tangent (tan δ with temperature for an AB05C8 sample (8% MWCNT content and 5:1 cross-link content). Measurement at 1Hz . . . . .	30
21	Effect of the DMA test frequency (1 Hz (continuous line) vs 10 Hz (dotted line)) on the loss and storage moduli and loss tangent of sample AB05C8. . . . .	31
22	Comparison of the storage, loss and complex moduli of the sample AB05C8 . . . . .	31
23	A schematic representation of the master curve E modulus-temperature that we propose for the PDMS/MWCNT nanocomposites. Three plateau regions are identified. . . . .	32
24	Variation of storage modulus with temperature for 5:1 cross-link density . . . . .	33
25	Variation of storage modulus with temperature for 10:1 Cross-link samples . . . . .	33
26	Variation of storage modulus with temperature for 15:1 Cross-link samples . . . . .	33
27	Variation of the storage modulus of the PDMS/MWCNT nanocomposites as a function of the cross-link content for each MWCNT load. . . . .	34
28	Variation of tanδ of the PDMS/MWCNT nanocomposites as a function of the MWCNT content for each cross-link content . . . . .	35
29	Variation of tan δ of the PDMS/MWCNT nanocomposites as a function of the cross-link content for each MWCNT load. . . . .	36
30	PDMS/carbon nanotube sample with two sets of deposited gold electrodes. Typical dimensions (width: 6 mm, thickness:1 mm, length: 2 cm). . . . .	38
31	Electrical conductivity of the PDMS/MWCNT nanocomposites as a function of the MWCNT load at room temperature. The line is a guide to the eye. . . . .	39
32	Picture of the setup for electrical resistance measurement with temperature variation. . . . .	40
33	Effect of the temperature on the resistance of samples AB10C4 and AB10C8. The lines are guides to the eye. . . . .	41
34	CeNTI . . . . .	45
35	IT . . . . .	45

# 1 Introduction

## 1.1 Motivation

Flexible electronics is an emerging field with a huge range of applications. It features electronic components and devices that can be wrapped around while retaining their functionality and are of great interest. Automotive, mobile and smart devices, health care and energy are examples of technological areas targeted by flexible electronics. Flexible electronics has advantages such as light-weight easy fabrication of prototypes, less waste of materials, production of a large area systems by using cheaper techniques (such as screen printing, roll to roll printing, knife coating), when comparing with the lithographic techniques used in the traditional semiconductors industry. In addition, material changes are easier to perform. There is a large number of materials, both small molecules and polymers, with a wide range of properties (such as electrical and optical properties, solubility).

Polymeric composites with nanofillers join two separate worlds and properties to create new materials with distinguished properties. In particular, the addition of nanofillers can change the mechanical and electrical properties of a given polymer. A polymeric material may be insulator but may become conductive if the proper amount of nanoconductive fillers is added. Not only electrical but also mechanical properties may be improved comparing to the pristine polymer.

Nanocomposites are materials with nanoscale structures aimed to improve the macroscopic properties of the polymers. Specific area of nanofillers is one of the advantages over bigger fillers. Due to its high specific surface area, there is a larger number of possible interactions between the nanofiller and polymeric matrix leading to a greater improvement of the final properties. This being said, polymer nanocomposites are an emerging area with diverse applications in very different fields. Due to their electrical and mechanical properties improvement, development of polymer nanocomposites for pressure sensors is one area that has raised attention. This project aimed the development of pressure sensors, using composites of polydimethylsiloxane with multi-walled carbon nanotubes (PDMS/MWCNT).



## 1.2 Pressure sensor

A sensor can be defined as a device or system that detects a stimulus and sends a signal to the operator, according to the received stimulus. The response may be an electrical signal or a change of the device colour (e.g. pH strips). Those stimuli can be pressure, temperature, humidity, magnetism, sound waves, specific compounds or pH. The electronic circuit can then be programmed to send a specific order to another components of the circuit when a specific output value is detected. For example, if we are growing cells we need to control the amount of glucose in the medium, otherwise cells may die [6]. We can build a sensor that measures the amount of glucose in the medium and alert the researcher only when it reaches a critical value. As previously mentioned, a sensor is a physical device that detects a physical event and sends an electrical signal to a circuit. However, not all physical quantities are easy to measure and so it is necessary to use transducers. Transducers are used to convert one energy form( ex: magnetism) into another(ex: voltage) that is easier for the operator to read. A sensor consists on the physical sensor itself and the transduction device. We can think on the physical sensor as the first step of data acquisition in the complete sensor [7] .

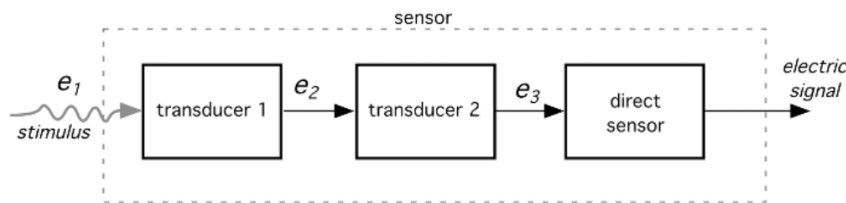


Figure 1: Simplified scheme of a Sensor

Pressure sensors are devices that are able to sense an exerting pressure on a specific area. There are various working principles for pressure sensors [8]. Capacitive sensors work by capacity changes of the device when pressure is applied or removed [9][10]. Piezoelectric sensors are constructed with piezoelectric materials. Piezoelectric materials generate a voltage different upon deformation and use its value to sense exerting pressure [11]. In this project, a PDMS/multiwall carbon nanotube nanocomposite for pressure sensing purposes was developed. PDMS/MWCNT nanocomposite changes its electrical resistance according to mechanical and thermal stimulus. For a fixed temperature and known area, the variation in electric resistance translates the pressure exerted on the composite. This project did not aim the development of the complete sensing device. It was focused on the analysis and characterization of PDMS/MWCNT composites, mainly addressing their mechanical and electrical properties, which can be used as the sensing element. PDMS, as will be detailed later, is prepared in situ, combining a pre-polymer and a cross-linking agent. The mechanical properties of the final polymeric network are dependent of the cross-linking content (that is, on the cross-linking degree). For simplicity, we will name the pre-polymer:cross-linking agent weight ratio as the “cross-link density”. In addition, being PDMS electrically insulator, the conductivity of the composite will depend on the MWCNT content.

### 1.3 Polymers and polymer nanocomposites

Polymer nanocomposites are a class of materials in which a nanometer-size material is dispersed in a polymeric matrix to combine the individual properties of each material to create a new one with superior characteristics. The content, dimension, shape, and surface chemistry of the filler will directly influence the final properties of the composite. Nanofillers have high specific surface area which is likely to lead to higher interactions (over larger fillers) with the polymeric matrix. When electrically conductive nanoparticles form networks inside the polymer, the composite may become electrically conductive. The development of nanotechnology techniques and nanomaterials increased the research and growth of nanocomposites with tunable properties (thermal and electrical conductivity, mechanical properties, biodegradability [12]). In general, polymeric materials are electrically insulators. The addition of electrically conductive nanoparticles (e.g. carbon black, graphene, carbon nanotubes, metallic nanoparticles), should they form networks (percolation paths) inside the polymer, may turn the composite into an electrically conductive material. Carbon nanotubes, due to their high aspect ratio, outstanding mechanical and electrical properties are interesting materials to improve the characteristics of this new class of materials. However, not only the properties of the fillers need to be addressed but also those of the polymeric matrix. For that, it is important to understand the mechanical and thermal behaviour of pristine polymers in order to better tune the properties of the final nanocomposite. A brief review of the properties of polymers is given below. The word polymer derives

from the words "poly", which means "many", and "monomer" that means "part". A polymer is therefore a high molecular weight molecule, made of repeat units ("mers"), which can be arranged as either a long-chain or as a sphere-like structure (called dendrimer). The term "macromolecule" is sometimes used to name them. The linear polymers can, in addition, be branched, cross-linked or made up of more complex structures. Polymers can be made of only one species (homopolymer) or different species (copolymer). Polymeric materials are known as viscoelastic materials as they combine viscous and elastic behaviours. Their mechanical properties depend on several factors such as molecular weight/chains length, molecular chemistry, temperature and stress/strain frequency. An elastic material is instantly deformed when force is applied (stores energy) but recovers its original shape upon force removal (releases energy). On the other hand, a viscous material flows upon applied stress and does not recover its original shape/form when the stress is removed. Its deformation is irreversible, opposite to an elastic material. Polymers viscoelastic properties can be characterized by the combination of a purely elastic and a purely viscous components [13] [14]. Maxwell model combines a purely elastic (Hookean spring) and a purely viscous (dashpot) elements, in series (Figure 4). When stress is applied, the purely elastic element is instantly deformed while the viscous one keeps deforming. Upon stress removal the deformation of the spring is recovered while the dashpot does not. Maxwell model is commonly used to describe stress relaxation behaviour in polymers. A constant strain is applied and the respective stress is measured with time [15]. A typical plot of a stress-relaxation experiment is shown in Figure 5.

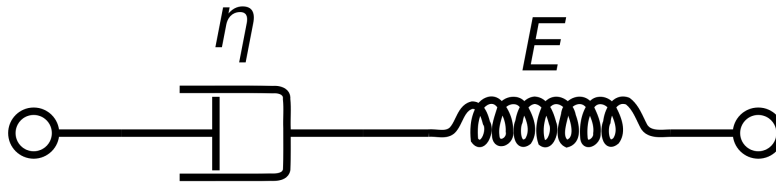


Figure 2: The Maxwell model

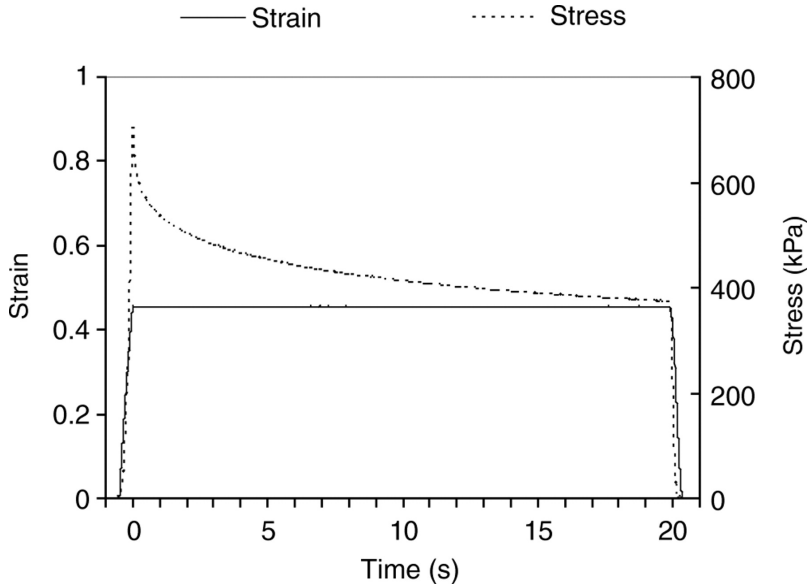


Figure 3: Stress relaxation

The mechanical properties of a polymer are dependent on its temperature. Glass transition temperature is a temperature at which a polymer transits from a glassy state to a rubbery state. Below glass transition temperature molecules are able to vibrate but do not move significantly. A polymer in glassy state is brittle and rigid. Above glass transition temperature, polymeric chains possess enough energy to move and the polymer becomes soft and more flexible [13]. At higher temperatures, melting may occur if the polymers are (semi)crystalline. Cross-linked polymers are formed when covalent or ionic bonds are created between polymeric chains. After cross-linking process, the molecules are connected to each other and chains mobility becomes more difficult. When cross-links are made of covalent bonds, melting does not occur. Evolution of elastic modulus with temperature is shown in Figure 4. In the glassy state, polymeric chains can not move significantly so its modulus is high. When temperature increases, polymeric chains increase their mobility due to thermal vibrations. That increase in mobility will soften the material, decreasing its elastic properties [13][15][14]. In Fig 4 it is possible to point out 3 distinct stages, a glassy, rubbery and viscous state. Dynamic mechanical analysis (DMA) is a technique in which dynamic properties are evaluated with temperature or frequency variations. DMA technique will be explained with more detail in chapter 1.10.2.

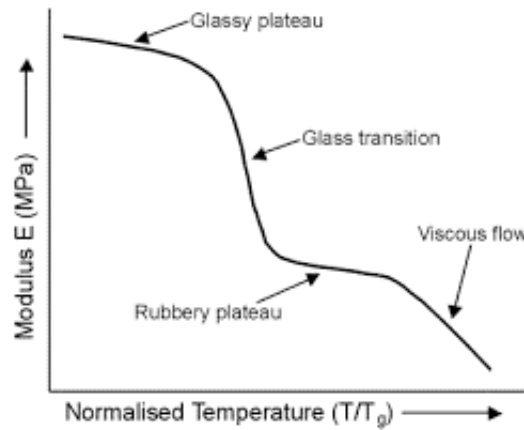


Figure 4: Schematic variation of the E/elastic modulus of a polymer with temperature.

## 1.4 Carbon allotropes

Carbon is a chemical element that has 6 electrons with the following electronic distribution:  $1s^2 2s^2 2p^2$ . It is a non-metallic element and due to its electronic distribution it is able to form up to 4 covalent bonds. Carbon is one of the most important elements on earth, not only because of its presence in almost every form of life but also due to its importance in materials engineering. Carbon is present in the air we expel (as carbon dioxide), in the food we eat (glucose, proteins), in our cells (lipids, proteins) and in a huge diversity of materials for building construction (steel), electronics (transistors, sensors), lubricants, tires reinforcements, cutting tools, etc. Diamond and graphite are the two most common carbon allotropes. The first was discovered in 1779 and graphite in 1789. Diamond is formed by  $sp^3$  hybridized carbon atoms (Figure 5) and displays the following properties:

- It is the best thermal conductor at room temperature; [16]
- Remarkable semiconductor properties when boron is added; [17]
- Hardest natural material found on earth :

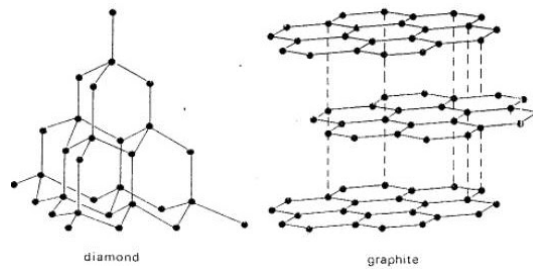


Figure 5: Diamond and graphite structure

Graphite on the other hand is composed of organized parallel planar monoatomic layers (known as graphene). Each layer has  $sp^2$  hybridized carbon atoms bonded to 3 other carbon atoms through  $\sigma$  bonds with 524 kJ/mol and 0.141 nm, forming a honeycomb-like structure, as represented in figure 5. The fourth valence electron located in the  $\pi$  orbital, is free to move and can create temporary dipole moments. The dipole moments created above and below the layer leads sheets packing through *van der Waals* bonds with 7 kJ/mol and approximately 0.335 nm distance. This being said, the general structure of graphite layers consists of directional  $\sigma$  bonds between neighbour carbon atoms and  $\pi$  bonds above and below the carbon sheet. The packing of this layers can occur in two forms: hexagonal (-ABABAB-) or rhombohedral (-ABCABC). Hexagonal is the most stable and it is found in natural graphite while rhombohedral is unstable. In both natural and synthetic graphite, rhombohedral content is less than 40%. From the bonding energy values presented above it is possible to highlight that the energy of the covalent bonding is approximately 75 times higher than the energy of *van der Waals* bonds between layers so graphene layers can slide past on another [18].

In 1996, Nobel Prize in Chemistry was awarded to Smalley, Kroto and Curl for the discovery of a new form of carbon, *buckminsterfullerene* in 1985.

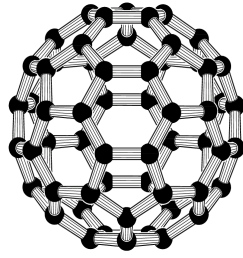


Figure 6: Buckminsterfullerene  $C_{60}$

*Buckminsterfullerene* is a ball-like molecule made of 60 carbon atoms bonded in hexagon and pentagon configurations and it was accidentally discovered when Kroto *et al.*, in 1985. found strange results in the mass spectra of evaporated carbon samples. Later, other similar molecules, fullerenes, were identified. The smallest one is  $C_{20}$  and the main fullerenes include  $C_{70}$ ,  $C_{72}$  and other larger molecules. In 1991, *Iijima, Sumio* discovered new forms of carbon, the multi walled carbon nanotubes, when trying to synthesize *buckminsterfullerene* using arc evaporation. Multi wall carbon nanotubes (MWCNT) were described as a tubular structure made of multiple carbon atom sheets (graphene) ranging from a few to few tens of nanometers in diameter. In 1993, a new type of carbon nanotube composed with only one rolled graphene sheet was reported. This new form of carbon was designated as single walled carbon nanotube (SWCNT). [19]

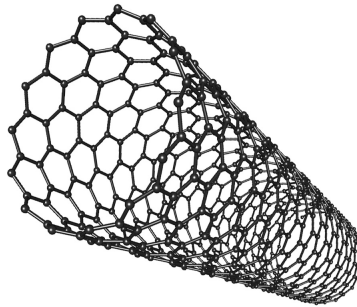
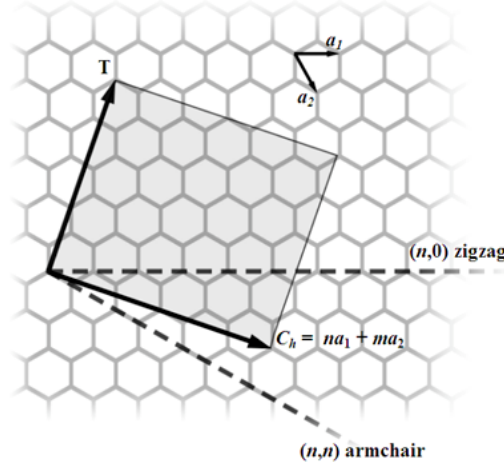


Figure 7: Single walled carbon nanotube

## 1.5 Carbon nanotubes

A carbon nanotube consists of a honeycomb lattice (graphene) rolled into a cylinder with length in the range of micrometers up to centimeters. There are two main categories, single walled (SWCNT) and multi walled (MWCNT). SWCNT can be defined as single rolled cylindrical graphene sheet giving rise to a tube-like structure with a diameter up to 20nm. Multi walled carbon nanotubes have more than one wall( two or more concentric nanotubes), diameters up to 300 nm and an average distance between layers of  $3.4\text{\AA}$  . Carbon nanotubes are sometimes considered as one dimensional structure due to high length to diameter ratio (aspect ratio). We can imagine that SWCNT result from the rolling of a graphene layer. Depending on the rolling mode, a SWCNT can be characterized by a pair of integers  $(n,m)$ , this corresponding to the coordinates of the rolling vector ( $C_h$ ) as shown below:



The  $(n,m)$  nanotube naming scheme can be thought of as a vector ( $C_h$ ) in an infinite graphene sheet that describes how to 'roll up' the graphene sheet to make the nanotube. T denotes the tube axis, and  $a_1$  and  $a_2$  are the unit vectors of graphene in real space. The optical and electrical properties of the SWCNT can be related such coordinates [18] [5] [20] [21]. If  $n = m$ , the nanotube is metallic; if  $(n - m)$  is a multiple of 3, then the nanotube is semiconducting with a very small band gap, otherwise the nanotube is a moderate semiconductor. A nanotube is chiral if is characterized by the pair  $(n,m)$  such that  $m > 0$  and  $m \neq 0$ . Then its mirror image, that is, its enantiomer is characterized by  $(m,n)$ , different from  $(n,m)$  [18] . An explosion of reports emerged after the discovery of carbon nanotubes and with that a better understanding of their properties. [20]. Carbon Nanotubes are among the strongest and most resilient materials in nature. Due to its strong  $sp^2$  bonds between carbon atoms, high tensile strength modules were expected. MWCNT were reported to withstand 150 GPa while SWCNT go up to 53 GPa. Carbon Nanotubes are very good conductors with conductivities reaching  $2 \times 10^7$  S/m [21] . However, as the conductivity values depend on several factors such as number of shells in case of MWCNT, diameter, chirality and aspect ratio [22] there is not a specific value for their conductivity. If we take a sample of SWCNT we will find that, some carbon nanotubes may be metallic and others semiconductors. Therefore, only an overall conductivity with the contribution of all carbon nanotubes types can be found. It was shown that the number of conductive paths of a carbon nanotube increases its conductivity and that the number of conductive paths increases with carbon nanotube diameter. Taking this into consideration, carbon nanotubes with bigger diameters have more conductive paths and so its conductivity increases. There is a strong research on methods to separate the metallic SWCNT from the semiconducting ones and, among these, to separate them by chirality. While metallic SWCNT are good to make conductive contacts, semiconducting SWCNT are required to prepare transistors.

However, the analysis becomes more complex when multi-walled carbon nanotubes are used due to the fact that each shell has its own characteristics. It was shown that in multi walled carbon nanotubes the inner shells(core of the nanotube) also contribute to the conductivity of the ensemble [23].In this study, authors removed sequentially the outermost shells of a MWCNT and recorded its voltage drop for different current inputs and observed contribution of the core even when 9 shells were removed. The variation of MWCNT electrical conductivity with temperature was also studied [23] [21]. It was shown that its response to temperature depends on the metallic/semiconducting content. Resistance increases for carbon nanotubes with metallic characteristics while for semi-conducting ones the opposite behaviour is observed [21]. Due to the fact that multi wall carbon nanotubes have multiple conducting walls contributing to the overall conductivity of the carbon nanotube, MWCNT were studied in this project. The funtionalization of carbon nanotubes was reported to be effective at increasing their dispersion. Functionalization with lateral groups such as carboxylic groups leads to a reduction of *Van der Walls* interactions between carbon nanotubes [5]. However , reduction of carbon nanotubes length and introduction of defects may occur upon functionalization , leading to a reduction of electrical conductivity[24].

Functionalization of carbon nanotubes was not performed in this project, however, should it take place, it should be performed in MWCNT and not in SWCNT. Functionalization affects mostly the outermost shell. In SWCNT, there is only one shell and the introduction of defects would greatly decrease its electrical properties. On the other hand, MWCNT have multiple shells and the introduction of defects has lower impact.[25].

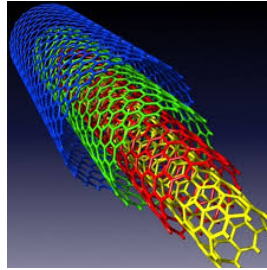


Figure 8: Multi walled carbon nanotube

## 1.6 PDMS

Polydimethylsiloxane (PDMS) is a silicon-based organic polymer and one of the most widely used in microfluidic devices and microelectromechanical systems (MEMS). PDMS has also been applied in sensors, electronic components and biomedical devices. PDMS is easy to process and synthesise, low cost, transparent and biocompatible [1] [26]. Due to its biocompatibility, PDMS has also been used as substrate for cell culture [27] [28]. It has also been a material of interest for nanocomposites. The chemical formula for PDMS is  $(\text{H}_3\text{C})\text{SiO}[\text{Si}(\text{CH}_3)_2\text{O}]_n-\text{Si}(\text{CH}_3)_3$  where  $n$  is the number of repetitive units. PDMS rheologic and mechanical properties depend on the number of repetitive monomers and chains termination. Formation of a PDMS networks is possible and is mediated by the addition of cross-linking agent that binds the PDMS chains, leading to the formation of elastomers known as silicon rubbers. The advantage of elastomers over thermoplastics in nanocomposites relies on their stability at high temperatures and ability to be deformed at high strain values within elastic regime. In this project, the main application of PDMS/Carbon nanotubes nanocomposite is as pressure sensor to be used at high temperatures (150-250°C). Therefore a polymer that is stable and maintains its elastic behaviour at that temperatures is required. PDMS Sylgard 184 was chosen as the polymeric matrix due to the fact that is stable at working temperatures and is widely used, easy to handle material, and shows adequate properties for the nanocomposite.

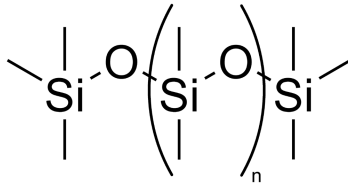


Figure 9: PDMS chemical structure

Sylgard<sup>®</sup> 184 is an elastomeric PDMS supplied by Sigma-Aldrich as a two-part kit consisting of a pre-polymer (Part A) and cross-linking agent (Part B). The recommended polymer/cross-linker mass ratio is 10:1 and curing time varies according to the curing temperature. Vinyl groups in part A react with Si-H groups in part B being catalysed by a Pt compound.

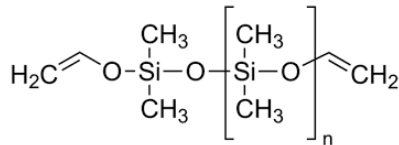


Figure 10: PDMS Sylgard 184

Mechanical properties of PDMS Sylgard<sup>®</sup> 184 were widely studied and it was demonstrated that curing temperature and cross-link ratio plays a crucial role in the final properties [26]. *Mata et al., 2006* tested 5 PDMS samples with increasing cross-linker concentration. Curing temperature was set to 95°C for 30 minutes followed by 24h at room temperature (25°C). Tensile tests demonstrate that Young Modulus does not show a monotonic dependence on the cross-linker content: it increases from 3.9 MPa [5.7% wt] to 10.8 MPa [14.3% wt] but decreased to 8.1 MPa [21.4%wt] and down to 4.0 MPa [42.9% wt]. This result show we may tune the mechanical properties of the final material upon selection of the appropriate cross-linker concentration. A similar study on the impact of curing temperature on final mechanical properties was also evaluated by Johnston et al [1]. Figure 13 sums up the results reported by these authors for PDMS Sylgard 184 with pre-polymer/cross-linker ratio of 10:1 wt.



**Table 2.** Variation of tensile test data with curing temperature.

Temperature (°C)	Average elongation (mm) [uncorrected]	Average failure load (kN)	Young's modulus (MPa)	Ultimate tensile strength (MPa)
25	93.1	92.34	$1.32 \pm 0.07$	$5.13 \pm 0.55$
100	76.4	112.5	$2.05 \pm 0.12$	$6.25 \pm 0.84$
125	66.2	137.7	$2.46 \pm 0.16$	$7.65 \pm 0.27$
150	63.4	94.32	$2.59 \pm 0.08$	$5.24 \pm 0.82$
200	49.5	63.18	$2.97 \pm 0.04$	$3.51 \pm 1.11$

**Table 3.** Variation of compressive properties of Sylgard 184 with curing temperature.

Temperature (°C)	Compressive modulus (MPa)	Ultimate compressive strength (MPa)
25	$186.9 \pm 5.39$	$51.7 \pm 9.60$
100	$148.9 \pm 5.47$	$40.1 \pm 4.30$
125	$137.7 \pm 2.82$	$36.8 \pm 3.84$
150	$136.1 \pm 2.68$	$28.4 \pm 4.46$
200	$117.8 \pm 2.17$	$31.4 \pm 2.04$

Figure 11: Elastic modulus for samples prepared at different curing temperatures [1]

Silicone elastomers are known for their high resistance to temperature and stretchability at room temperature. Thermogravimetry analysis on PDMS Sygard 184 demonstrates its stability up to approximately 300°C [29]. The good mechanical properties of PDMS Sylgard 184, its high thermal stability and easy fabrication process supported our choice of this material as the polymeric matrix of the nanocomposites.

## 1.7 Polymer/carbon nanotubes nanocomposites

In view of the above mentioned characteristics of carbon nanotubes, they have been used to prepare nanocomposites with various polymers to obtain new or improved properties. 1% wt of MWCNT reinforcement in polystyrene matrix was shown to be effective in increasing elastic modulus and tensile strength by 42% and 25%, respectively [30]. Other polymers such as epoxy resins [31], PVA [32] and PMMA [33] were also tested.

In the present work, a composite of PDMS/carbon nanotube was developed in order to fabricate a flexible conductor, whose electrical resistance that changes its resistance according to mechanical stimulus. This work is motivated not only by the expected properties but also by previous works with this composite that shows very good results. *Engel et al* developed a capacitive sensor dispersing multi-walled carbon nanotubes with diameters of 50-100nm and length of 1-5micrometer in PDMS Sylgard 184 and in polyurethane [34]. It was observed that the percolation threshold is 5 times lower for PDMS than polyurethane (2% and 10% respectively). In addition, for 5% and 10% the sheet resistance is approximately 1000 and 150 ohms/square, respectively. *Wu et al, 2008* reported the mechanical and electrical properties of PDMS/MWCN composites for different concentrations, curing time and temperature [35]. It was observed that when MWCNT content increases, the elastic modulus and stress at specific strain values of the resulting composite also increases. The curing temperature was also studied, however not significant conclusion can be taken from this experiment since only 2 curing temperatures were evaluated. In spite of that, elastic modulus increased for all concentrations when curing temperature increased from 100 to 150°C.

Flexible electronics is prone to large scale production. A certain polymer intrinsically (semi)conducting with conducting particles can be easily spread in a surface and acquire a certain shape. Screen printing of PDMS/MWCNT was proved to be effective in producing flexible electronics [2]. *Khan et al* tested PDMS composites with three carbon nanotube concentrations, 3, 4 and 5%. It was reported a decrease in resistance from 40 kOhm to almost 1 kOhm was reported when concentration increases from 3 to 5%. A resistance when pressure is applied was also evaluated [2] (Fig 14).

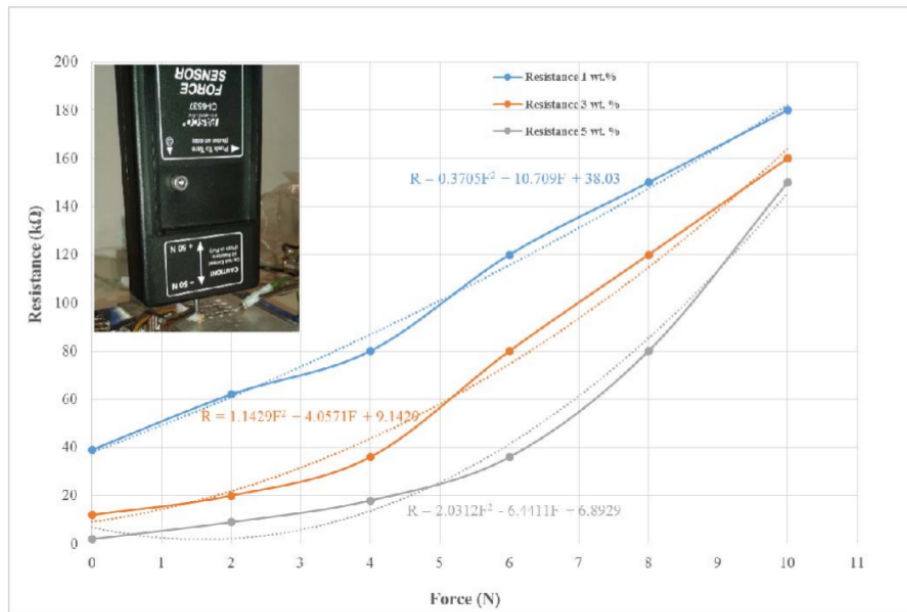


Figure 12: Resistance Vs Force [2]

Another recent and interesting article demonstrated the potential of PDMS/MEP/MWCNT for wearable electronics [3]. MEP(methyl group-terminated PDMS) was used to increase the dispersion of the MWCN in the polymeric matrix. *Kim et al* studied the resistance variation of PDMS/MEP/MWCN when 10.000 cyclic strains were applied [3]. Concentrations from 0% to 20% were studied and conductivity values of  $2.281 \pm 0.137$  S/cm and  $0.003 \pm 0.001$  S/cm for 20% and 1% respectively were reported. Cyclic strains with resistance measurements showed no significant changes after 10000 cycles for 4%,8% and 12% samples (Figure 13).

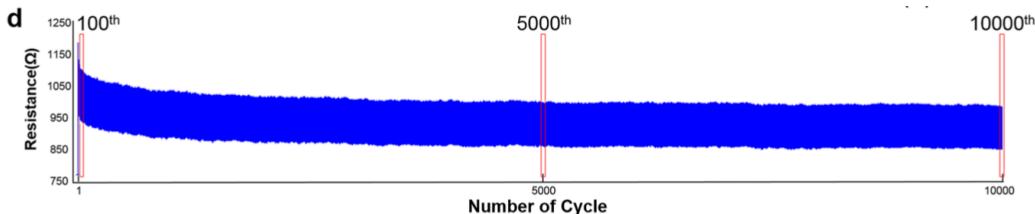


Figure 13: Resistance response with cyclic strain for a 4% MWCNT containing PDMS/MEP/MWCNT composite [3]

The electrical conductivity of a polymer/carbon nanotube composite is dependent on the network formed by the carbon nanotubes upon dispersion within the polymeric matrix. Carbon nanotubes may contact each other or be separated by few nanometers. For carbon nanotubes separated by few nanometers, tunneling needs to be considered as an electric conducting mechanism. If more electrical conductive paths exists in the network, a less resistive material is obtained. As stated before, when carbon nanotube loading increases, the electric resistivity of the material decreases, which can be explained by the formation of a conductive network with more contacts or shorter distance between nanotubes. [36] [37] [38] [39]. Percolation threshold of carbon nanotubes composites may vary according to polymers properties, processing techniques or carbon nanotube type. Percolation threshold can be defined as the concentration at which a sharp increase in electric properties is observed ( Fig 16 and 17 ) [4].

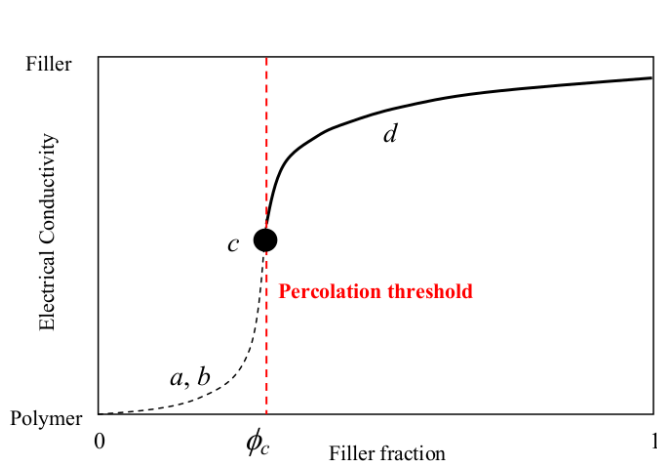


Figure 14: Percolation threshold [4]

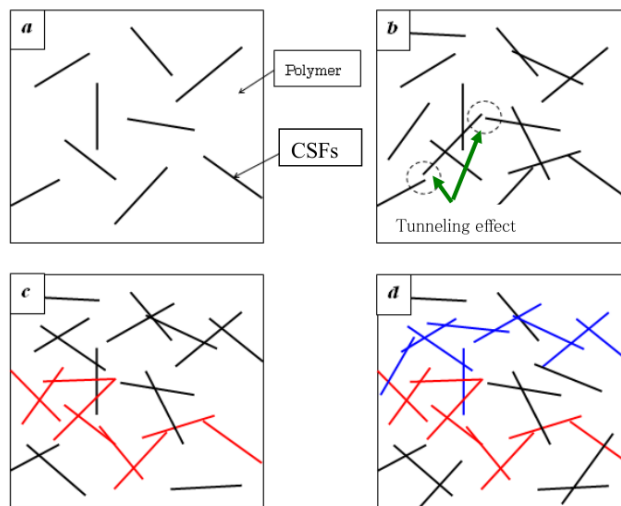


Figure 15: Conductive network formation [4]

Percolation threshold of 0.0025% [40] and 0.004% [41] for epoxy resins/MWCNT were reported. Some key factors may play an important role in the final electrical properties of the composites. It was observed that maximum dispersion of Carbon Nanotubes is not desired since the distance between carbon nanotubes would increase leading to lower electrical conductivity. On the other hand, agglomeration of nanotubes decreases the overall electrical conductivity of the composite due the formation of localized conductive networks. A balance between dispersion and agglomeration is necessary in order to achieve higher electric conductivity. The formation of an encapsulating

layer surrounding the carbon nanotubes that can act as barrier for contacts between carbon nanotubes, lowering its electrical conductivity was reported [42] [43]. An interesting study compared the percolation threshold of dispersed and agglomerated carbon nanotubes . 0.11 wt.% and 0.068 wt.% percolation threshold were obtained for films with uniformly dispersed and agglomerated carbon nanotubes, respectively [44]. In summary, a good dispersion is desired but some agglomeration may be beneficial for the composite’s electrical conductivity.[4] Polymer carbon nanotube interaction needs to be balanced, because high interaction may increase dispersion but the development of a polymeric capsule surrounding the carbon nanotube may occur. For a better understanding of the dispersion of fillers in polymeric matrix, simulations comparing the dispersion of aluminium oxide , carbon fibers, graphene nanopellets(GNP) and carbon nanotubes(CN) were performed. For the same weight percentage , *Ma et al* observed that a higher dispersion was obtained for carbon nanotubes . This result provides a good reason to develop nanocomposites with carbon nanotubes, as these can form a better electric conducting network which may increase its electrical conductivity comparing to others fillers [5].

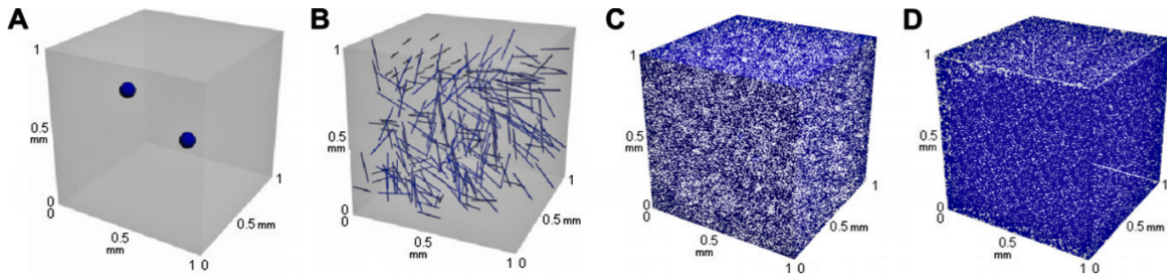


Figure 16: Distribution of micro- and nano-scale fillers of the same 0.1 vol.% in a reference volume of 1 mm<sup>3</sup> (A: Al<sub>2</sub>O<sub>3</sub> particle; B: carbon fiber; C: GNP; D: CN). [5]

The main purpose of the development of PDMS/carbon nanotubes nanocomposite is to use them in pressure sensors, assessing their ability to sense pressure. When a polymer/carbon nanotube composite is stretched, the distance between carbon nanotubes increases and some conductive paths are disrupted, resulting in a less electrically conductive material [45]. This change in electrical conductivity can, therefore, be used to sense pressure in a known area. Upon mechanical deformation, the conductivity of the nanocomposite changes due to the increased distance between carbon nanotubes. It is also important to assess the changes in electrical conductivity of the nanocomposite upon temperature increase. *Zeng et al* studied the properties of High Density Polyethylene(HDPE)/MWCNT for 5, 8,10,12 and 15 wt% CNT content. A drastic decrease of HDPE/Carbon Nanotube electric resistivity with increment of carbon nanotubes loading was observed, as expected . *Zeng et al* , reported also a slow increase of electrical resistivity when temperature was raised from 40°C to 120°C with a sharp increase in resistivity for higher temperatures. Increase in electrical resistivity upon temperature, typically found in metals, may, in this case, be due to thermal expansion. When temperature increases, the polymer matrix expands and the distance between carbon nanotubes increases affecting their ability to conduct electronic charged carries. Different results was observed with PEEK/Carbon nanotubes nanocomposites [46]. Upon temperature increase from 20°C to 140°C , the electrical conductivity increased approximately 6 times for 8%, 9% and 10% carbon nanotube loading. Thermal expansion plays a key role in electrical properties upon temperature increase. The higher the expansion coefficient of polymeric nanocomposites the faster is expected the electrical conductivity to decrease.

The effect of temperature on PDMS/MWCNT nanocomposite stability was also tested [47]. Thermal gravimetry analysis was performed from 0°C to 800°C. It was verified that the temperature at which a 10% weight loss occurs increases when carbon nanotube loading increases from 0,5% to 2,0%. Due to the high thermal conductivity of carbon nanotubes, the thermal stability of the nanocomposite is improved.

### 1.7.1 PDMS/carbon nanotube preparation

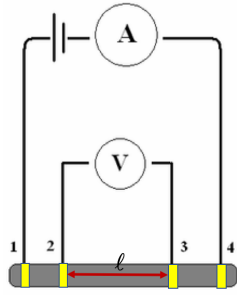
*In situ* polymerization, sol-gel and direct mixing of a polymer and nanofillers are suitable used methods to prepare polymer nanocomposites. In *in situ* polymerization, nanoparticles are spread out in a liquid monomer until an homogeneous solution is obtained. Polymerization occurs upon addition of an initiator and exposure to heat or radiation. This method is simple and fast and is used to produce large polymeric nanocomposites thin films. Sol-gel process involves the formation of a network by polymerization reaction. Solid nanoparticles are dispersed (sol phase) in a monomer solution and during polymerization a network between phases is formed (gel). Solvent evaporation is then performed. Direct mixing can be performed with addition of solvents or not. With solvent method, nanoparticles and polymer are dispersed in a common solvent. Upon complete homogenization, solvent is evaporated [48] [49]. One of the objectives of this project, relies on the development of a conductive PDMS/carbon nanotube composite that can be fast and easily produced in large thin films. This being said, direct dispersion of carbon nanotubes in PDMS with a common solvent is a viable option that as shown good results. Dispersion of carbon nanotubes with PDMS in toluene, chloroform, tetrahydrofuran (THF) and dimethylformamide (DMF) was studied [50]. First, dispersion of multiwall carbon nanotubes was tested without PDMS. DMF and THF showed the best results 70 hours after sonication. In order to increase homogeneity, carbon nanotubes can be first dispersed in a solvent and PDMS is added when good carbon nanotube dispersion is observed. Upon addition of PDMS, chloroform demonstrated the best dispersion results. Dispersion of pristine multiwall carbon nanotubes with 7 different organic solvents was tested [51]. Acetone, THF, dichloromethane and *n*-methyl-2-pyrrolidone (NMP) demonstrated the best dispersion results.

In order to obtain good dispersion, a common solvent will be necessary. Isopropanol (IPA) is a partially-solvent of PDMS and demonstrated good results upon single wall carbon nanotube dispersion [52]. *Ramalingame et al., 2017* compared the impact on electric properties when dispersion of PDMS and multiwall carbon nanotubes is performed in isopropanol, chloroform, THF and toluene [53]. Isopropanol demonstrated the best dispersion and electric results. Isopropanol was the selected solvent for this project since it is available at the laboratory, it has a hydrophobic structure able to attach carbon nanotubes (reducing interaction between CN), air bubbles are easily removed (which is important since PDMS easily traps air bubbles) and is less volatile than dichloromethane and chloroform. In order to reduce environmental impact and health problems of the operator, less toxic solvents need to be used. Isopropanol is less toxic than toluene, dichloromethane and chloroform supporting its choice. Isopropanol boiling point is 82.5°C, density of 786 kg/m<sup>3</sup> and 60.1 g/mol molar mass. The boiling point of 82.5°C allows more control over evaporation process comparing to more volatile solvents. Taking everything in consideration, isopropanol was used as solvent in PDMS/MWCNT preparation.

## 1.8 Techniques

### 1.8.1 Electrical Characterization

The electrical conductivity of the PDMS/MWCNT nanocomposites was determined using both the four-contacts and two-contacts probes methods. The four-contact method consists on placing four metallic contacts, usually made of thermally deposited gold, that cross the entire section of the sample, as shown in Scheme 1. A constant current ( $i$ ) is injected between contacts 1 and 4 and the voltage drop ( $\Delta V$ ) between the two inner contacts (2 and 3) is measured with a voltmeter. With this method, contacts resistance is eliminated resulting in more accurate measurement. Using equation 4 , the resistivity of the material is obtained [54].



Scheme 1: The four-contacts method to determine a sample's electrical conductivity

$$\rho = R \frac{l}{t * w} \quad (1)$$

Where  $R = \frac{\Delta V}{i}$

- $\rho(\Omega.m)$  = Electric resistivity ;
- $t$  = Thickness;
- $w$  = Width, so that  $t*w$  gives the cross-section of the sample ;
- $l$  = Length(distance between the two inner contacts ;

There is a similar method, named the four-point method (or Kelvin technique), mostly used to determine the resistivity of thin films, where 4 colinear probes, with equal separation ( $l$ ) between them, are made to contact the material's surface (see Figure 19).

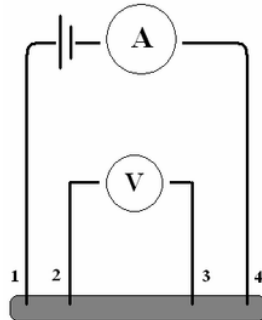


Figure 17: Four Point Probe Method

In this case, the resistivity of the film, is calculated as  $\rho = R_s t = \frac{t\pi}{\ln 2} \frac{\Delta V}{i}$  provided that the material being tested is no thicker than 40% of the spacing between the probes, and the lateral size of the sample is sufficiently large. Should these two conditions not be met, then a geometric correction has to be made. The two-contact probe method consists in placing only two contacts on the sample of interest in order to measure the electrical properties. The two probes inject current and measure the voltage difference at the same time (as an ohmmeter does). Despite the error induced by the contacts resistance, (which is more relevant for highly conductive samples) the advantage of this methods relies on its simplicity. For the application as pressure sensor, with the sensing process relying on the variation of the sample's electrical resistance upon application of a given stress, the two-point probe method is preferred. Despite the above mentioned lower accuracy of this method, as the samples resistance is usually very large, no significant differences on the resistance variations are expected. The accuracy of the method will depend on the negligible effect of the pressure-induced deformation of the samples on the contact resistance and possible degradation of the contacts quality.

### 1.8.2 Mechanical Properties

**Dynamic Mechanical Analysis** is a common technique to evaluate the viscoelastic behaviour of materials. A sinusoidal stress is applied and the sinusoidal strain is measured along with the phase angle ( $\delta$ ). DMA technique allows the analysis of the mechanical response as function of stress frequency, temperature and time. Viscoelastic materials exhibit a combination of elastic and viscous properties. The analysis of their behaviour is usually made using a combination of two ideal components: a pure elastic element (Hookean Spring)(equation 4) and a pure viscous element( equation 5 ). This being said, the mechanical properties of viscoelastic materials are dependent of the balance between elastic and viscous content. The phase-angle is the phase difference that exists between the applied stress and the respective strain. As equation 6 and 7 suggests, the phase-angle will be 0 if the material is purely elastic and  $\frac{\pi}{2}$  for purely viscous materials. Since viscoelastic materials has properties that are between those of a pure elastic and of pure viscous materials, their phase-angle value will range from 0 to  $\frac{\pi}{2}$  and translates the elastic and viscous content of the material [55][13] [14] [56].

Equations 6 and 7 hold when a viscoelastic material is subjected to a sinusoidal stress-strain experiment.

$$\sigma(t) = \sigma_0 \sin(tw + \delta) \quad (2)$$

$$\epsilon(t) = \epsilon_0 \sin(tw) \quad (3)$$

$t(s)$  = Time;  
 $w(Hz)$  = Strain frequency;  
 $\delta$  = Phase lag;  
 $\epsilon$  = Strain;  
 $\sigma(N)$  = Tension;

Purely elastic solids are instantly deformed when stress is applied. A spring that obeys Hooks law is then used as perfect elastic model :

$$\sigma(t) = E\epsilon(t) \quad (4)$$

where E is the Young or elasticity modulus. On the other hand, a dashpot with a newtonian fluid is used to describe the behaviour of purely viscous materials:

$$\sigma(t) = \eta\dot{\epsilon} \Leftrightarrow \sigma(t) = \eta[d\epsilon/dt] \quad (5)$$

where  $\eta$  is the fluid viscosity. When a purely elastic material is subjected to a sinusoidal stress , its phase-angle will be 0. This can be demonstrated if we combine equation (4) with equations (2) and (3):

$$\sigma(t) = E\epsilon(t) \Rightarrow \sigma_0 \sin(tw + \delta) = E\epsilon_0 \sin(tw) \Rightarrow \delta = 0 \quad (6)$$

If we combine equation (5) with equations (2) and (3), we obtain that, when a purely viscous material is subjected to a sinusoidal stress, a phase-angle of  $\frac{\pi}{2}$  is observed:

$$\sigma(t) = \eta \frac{d\epsilon}{dt} \Rightarrow \sigma_0 \sin(tw + \delta) = \eta\epsilon_0 w \cos(wt) \Rightarrow \delta = \frac{\pi}{2} \quad (7)$$

To facilitate the analysis of the elastic and viscous contributions, we can write the imposed strain as a complex oscillating function

$$\epsilon^*(t) = \epsilon_0 e^{iwt}$$

so that the corresponding stress, would be

$$\sigma^*(t) = \sigma_0 e^{(iwt+\delta)}$$

The real strain and stress are, respectively, the real part of the corresponding complex quantities.

For viscoelastic materials, there is not only one elastic modulus but a complex modulus that has the contribution of loss and storage modulus, viscous and elastic phases respectively.



$$E^* = \frac{\sigma^*(t)}{\epsilon^*(t)} = \frac{\sigma_0 e^{i\omega t + \delta}}{\epsilon_0 e^{i\omega t}} = \frac{\sigma_0 e^{\delta}}{\epsilon_0} = \frac{\sigma_0}{\epsilon_0} (\cos \delta + i \sin \delta) = E' + iE'' \quad (8)$$

In the above equation,

$$E' = \frac{\sigma_0 \cos \delta}{\epsilon_0}$$

is known as storage modulus (or dynamic modulus of elasticity) and

$$E'' = \frac{\sigma_0 \sin \delta}{\epsilon_0}$$

is known as loss modulus.  $\delta$  is known as the loss angle. The storage and loss moduli measure the stored energy, representing the elastic portion, and the energy dissipated as heat, representing the viscous portion, respectively. The ratio between the loss and storage moduli is defined as  $\tan \delta$  or loss tangent, which provides a measure of energy dissipation in the material.

$$\tan \delta = \frac{E''}{E'} = \frac{\sin \delta}{\cos \delta}$$

$\tan \delta$  ranges from zero, for an ideal elastic solid, to infinity, for an ideal liquid.

In polymers, the loss modulus and the loss tangent are mainly determined by the type and intensity of molecular motion. Higher values of  $\tan \delta$ , mean that the viscous component surpasses the elastic one. “Unfreezing” of almost every new type of molecular motion results in the appearance of maxima on the temperature or frequency dependence of the loss tangent. This way, following the temperature dependence of the  $\tan \delta$  allows us to identify a multitude of molecular relaxation processes. Peaks in  $\tan \delta$  will identify transition temperatures, which, in amorphous polymers, are related to molecular relaxation processes, being the glass transition temperature the most relevant, while for crystalline polymers the melting temperature will also be detected. Figure 18 shows the basic temperature transitions in an amorphous polymer [57]. The peaks are identified as  $\alpha$ ,  $\beta$ ,  $\gamma$  and  $\delta$  starting from the most intense, high temperature one. The peak of the main relaxation ( $\alpha$ ), corresponding to a maximum peak of the losses, is attributed to the glass transition. This the transition that has a more dramatic effect on the molecular motion.

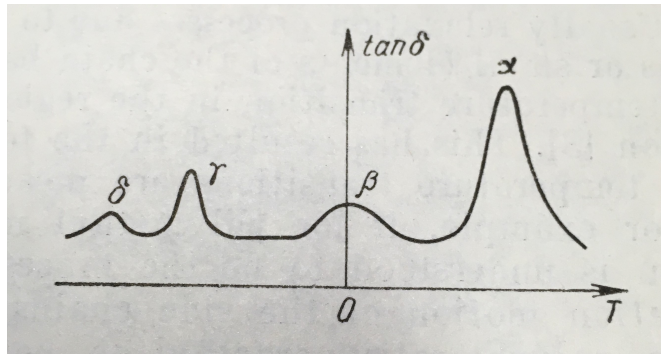


Figure 18: Transitions in amorphous polymers as detected by the loss tangent (Reproduced from “Acoustic Methods of Investigating Polymers”, I. Perepechko (translated by G. Leib), Mir Publishers, Moscow, 1975)

Peak  $\beta$  is usually associated to relaxation processes due to motion of sides groups or small elements of the chain backbone. The processes related to  $\gamma$  and  $\delta$  peaks may have a multitude of origins. For instance, gamma-relaxation can be related to motion of four or more  $\text{CH}_2$  or  $\text{CF}_2$  groups, while the delta-relaxation may be related to motion of terminal and separate atomic groups.

In semicrystalline polymers, between the liquid nitrogen temperature and their melting temperature,  $T_m$ , at least three relaxation processes are often found (see Figure 21). At  $T_m$  a maximum  $\tan \delta$  is observed, followed by an  $\alpha_c$  peak at lower temperatures, which, if present, is related to relaxation within the crystalline phase. The peak III represents the glass transition within the amorphous phase. The low temperature II peak is related to a relaxation

within the amorphous phase, although it may also have a contribution from the crystalline phase. Other peaks, at lower temperatures, may be detected. This sequence of peaks is shown, below, in Figure 19.

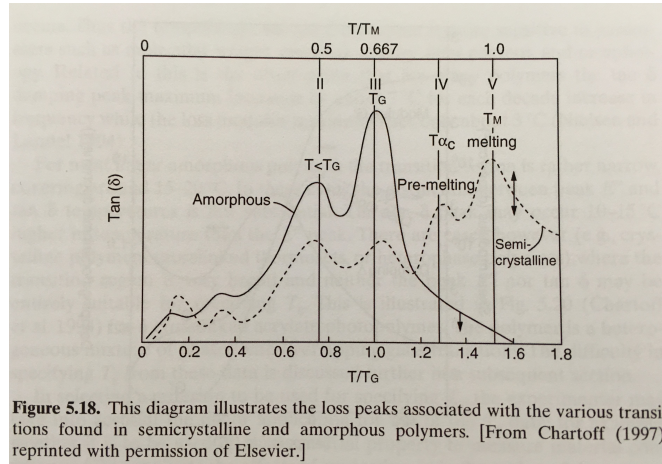


Figure 19: Comparison of the loss peaks in semicrystalline and amorphous polymers. Reproduced from “Thermal Analysis of Polymers-Fundamentals and applications”, Joseph D. Menczel and R. Bruce Prime, eds, Wiley, 2009

The position of the glass transition peak in semicrystalline polymers depends on the degree of crystallinity and morphology of the polymer. Secondary transitions are influenced by various factors, such as diluents, moisture, fillers, pigments, and nature and density of the cross-links.

## 1.9 Research Objectives

- 1) Effect of carbon nanotubes loading and cross-linking density on the dynamic mechanical properties of the composites;
- 2) Effect of carbon nanotubes loading on the electrical properties;
- 3) Variation of the electrical resistance with temperature;
- 4) Effect of cross-linking density and carbon nanotubes loading on the electrical properties;
- 5) Effect of cyclic stress and temperature on the electrical conductivity of PDMS/MWCNT composites

## 1.10 Research Strategy

In order to address the points raised above, the following strategy was pursued :

- 1) Dynamic Mechanical Analysis (DMA) was performed on 12 different samples. To analyse the effect of cross-linking density, 3 different cross-linking degrees were tested. To evaluate the effect of carbon nanotubes loading, for each cross-linking density, 4 different carbon nanotubes contents were tested.
- 2) Electrical resistance assessed by the four-point probe method on 4 samples with 4, 6, 8 and 10% carbon nanotubes loading. “Cross-link density” of all sample was 10:1
- 3) Two-point probe method was used to assess the electrical resistance on 2 samples with 4 and 8% carbon nanotubes loading. Study of the variation of electric resistance upon increase of temperature.
- 4) Electric resistance measurements using the two-point probe method on 12 samples with 3 different cross-link density and 4 different cross-link densities, each.
- 5) Two-point probe method was performed before and after DMA studies in order to assess the effect of cyclic tension and temperature on the electrical properties.

## 2 PDMS/carbon nanotube preparation protocol

### 2.1 Materials

PDMS Sylgard 184 was purchased as two part kit from Dow Chemicals. Multi Wall Carbon Nanotubes with 110-170nm of diameter, 5-9 micrometer length and purity above 90% were purchased from Sygma Aldrich.

### 2.2 Samples Preparation and Characterization

In the present work, a composite of PDMS/MWCNT were developed in order to build a flexible(elastomeric) conductor. PDMS/MWCNT nanocomposites were synthesised using PDMS Sylgard 184 Elastomer Kit, which is composed by a silicon elastomer base(Part A) and PDMS curing agent(Part B). Since it is important to understand how cross-link degrees affect the formation of MWCNT networks and the respective mechanical properties, 3 cross-link degrees were studied. According to PDMS Sylgard 184 data sheet [58] , the recommended ratio Part A:Part B is 10:1. The notation that will be used for cross-link degree of different samples is the same as presented in PDMS Sylgard 184 data sheet: Part A:Part B.

The chosen procedure(Procedure 1) for PDMS/Carbon Nanotubes synthesis is the following:

- Dispersion of MWCNT in Isopropanol(S1) in ultrasonds for 30 minutes. MWCNT/IPA ratio of 1:50 %wt. ;
- Dispersion of PDMS Part A in Isopropanol(S2) with magnetic stirrer for 1 hour (PDMS/IPA ratio of 1:2 wt);
- Mixture of S1 with S2, increase temperature to 60°C and agitate with a magnetic stirrer;
- Wait until Isopropanol evaporates;
- Cool down the resulting solution, add Part B and mix the solution;
- Pour the "solution" into a mold or spread with a knife on a flat surface;
- Put the samples in a vacuum chamber for 1 hour at room temperature;
- Set furnace temperature to 80°C, insert samples and wait 2 hours(under ambient pressure);

In order to prepare a reasonable amount of PDMS/MWCNT films, 1 and 2 grams of PDMS Part A were used in each thin film. Each PDMS/Carbon Nanotube film was then cutted into samples with various sizes in order to measure its electric and mechanical properties. Since it is important to understand how cross-link degrees affect the formation of MWCNT networks and the respective mechanical properties, 3 cross-link degrees were studied.

To assess the mechanical behaviour of PDMS/MWCNT nanocomposites, dynamic mechanical analysis was performed. The Dynamic Mechanical Analysis of PDMS/multiwalled carbon nanotubes composites was performed on a Perkin Elmer Dynamic Mechanical Analysis 8000 in tension mode with sinusoidal strain input. The range of temperatures is from approximately -130C to 250C. The minimum temperature was not the same for all specimens due to liquid nitrogen and equipment limitations. However, it was possible to achieve a common minimum temperature of -120C for all specimens. Two frequencies, 1Hz and 10Hz, were tested at the same time. Heating rate was 3°C/min. Storage modulus( $E'$ ), loss modulus( $E''$ ) and  $\tan \delta$  of each specimen were then obtained.

The evaluation of the electrical resistivity of the samples using the four contacts method, involved the thermal deposition of gold stripes (ca. 40-50 nm thick) through a shadow mask in an Edwards Coating System E 306A. Current was applied with a Keithley 2400 Source Measure Unit and the voltage drop was measured with an Agilent 34401A Multimeter. The evaluation of the electrical resistivity of the samples using the two contacts method was measured with Agilent 34401A Multimeter.

### 3 Results

The samples prepared in §2.2, were identified as shown below (Table 1)

Table 1: Samples identification according to their cross-linker and MWCNT content

Part A: Part B \ CN weight %	4%	6%	8%	10%
5:1	AB05C4	AB05C6	AB05C8	AB05C10
10:1	AB10C4	AB10C6	AB10C8	AB10C10
15:1	AB15C4	AB15C6	AB15C8	AB15C10

The properties of these nanocomposites, namely:

1. Dynamic mechanical properties of all PDMS/carbon nanotubes samples
2. Electrical properties of PDMS/MWCNT composites:
  - Electrical conductivity at room temperature (Samples AB10C4, AB10C6, AB10C8 and AB10C10);
  - Variation of electrical resistance of 2 samples (AB10C4 and AB10C8 ) with temperature;
  - Electrical properties of all 12 samples before and after Dynamic Mechanical Analysis ;
  - Electrical properties of 4 samples ( AB10C4, AB10C6, AB10C8 , AB10C10 ) under stress;

are presented in this chapter.

### 3.1 Dynamic Mechanical Analysis of PDMS/MWCNT nanocomposite

In order to assess the role of MWCNT content and cross-link content on the mechanical properties, Dynamic Mechanical Analysis (DMA) was performed on all twelve PDMS/MWCNT samples (identified in Table 1).

Figure 20 shows typical DMA results, specifically for the AB05C8 sample, obtained at 1Hz.

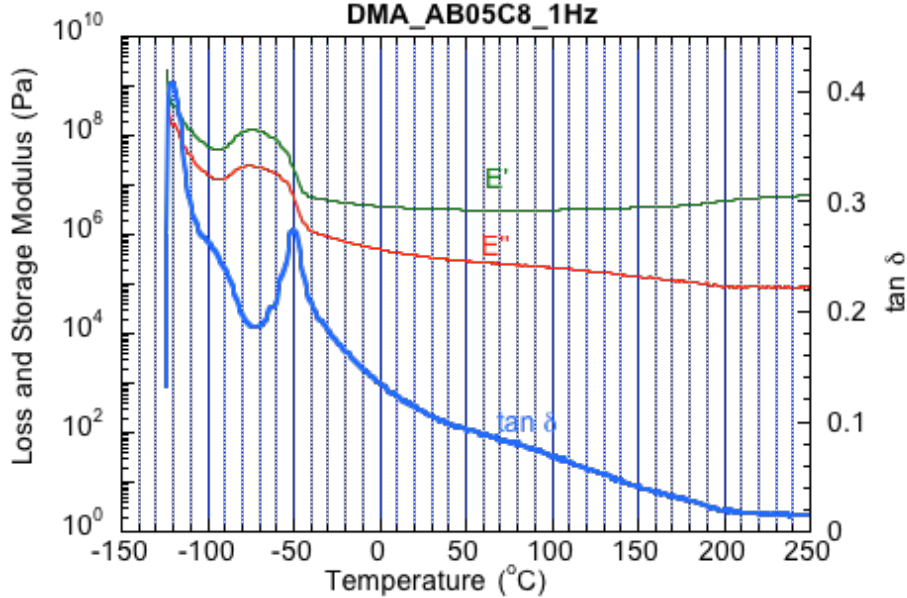


Figure 20: Variation of storage modulus ( $E'$ ), loss modulus ( $E''$ ) and loss tangent ( $\tan \delta$ ) with temperature for an AB05C8 sample (8% MWCNT content and 5:1 cross-link content). Measurement at 1Hz

We have discussed above that the highest intensity peak of the loss tangent corresponds to the glass transition, in amorphous polymers, or to the melting transition in semicrystalline polymers and that no peaks are detected above  $T_g$  (in case of the amorphous polymers) nor above  $T_m$  (in case of the semicrystalline polymers). The results in Figure 20 show that  $E'$  and  $E''$  follow a similar variation with the temperature, nearly stabilizing above ca.  $-40^\circ\text{C}$ . As illustrated by the  $\tan \delta$  two main transitions are identified. One around  $-122^\circ\text{C}$  and the second one at around  $-50^\circ\text{C}$ . The transition at ca.  $-122^\circ\text{C}$  is identified as the glass transition, while the transition at ca.  $-50^\circ\text{C}$  is associated to the melting process. It has been reported [59] that cross-linked PDMS is a semicrystalline polymer network. The loss modulus is lower than the storage modulus across the entire temperature range, evidencing that the elastic component prevails over the viscous component. It should be noted that the determination of  $T_g$ , under the present conditions, has a significant error as this temperature close to the lower limit of the accessible temperature interval. At  $50^\circ\text{C}$  the storage and loss moduli are  $3.174 \times 10^6$  Pa and  $2.956 \times 10^5$  Pa, respectively. The fact that both  $E'$  and  $E''$  stabilize after the melting process is a signature of the structure of the material (polymeric network). The feature in both  $E'$  and  $E''$  curves below the melting (at ca.  $-90^\circ\text{C}$ ), consisting on a dip, is common to all samples. We have two possible explanations for this observation. The first is to consider that the dip is associated to a non-identified molecular relaxation process (a pre-melting process). The second one, which we consider more likely, is that the trend is not the observation of the dip but the sudden increase of both  $E'$  and  $E''$  above ca.  $-90^\circ\text{C}$  and this increase being associated to a crystallization of the sample. When the samples are cooled to the lowest temperature it is likely that the samples reach a metastable state, without time to reach the proper crystallization. This is a well-known observation in polymers. Semicrystalline polymers can be obtained as amorphous materials if they are fast cooled (quenched) from the “melt” to a low temperature, preventing the polymer chains to reorganize from the melt into an ordered state. Figure 21 compares the DMA results obtained for sample AB05C8 at 1Hz (shown in Figure 20) with those obtained at 10Hz. We find that the results at 10Hz, corresponding to shorter relaxation times, lead to a shift of the curves to higher temperature and to slightly higher values of both the storage and loss moduli. In the remaining of the text we will refer only to the DMA data obtained at 1Hz.

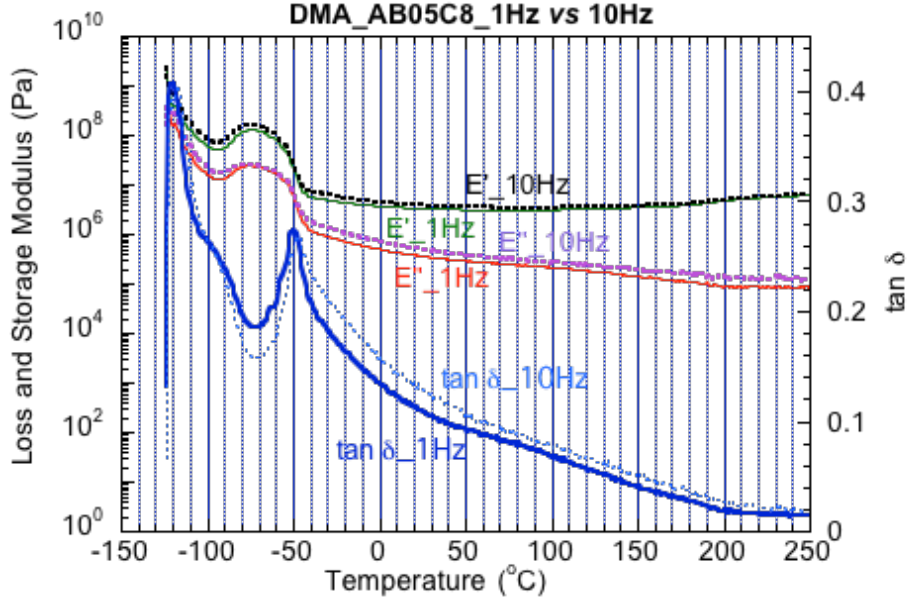


Figure 21: Effect of the DMA test frequency (1 Hz (continuous line) vs 10 Hz (dotted line)) on the loss and storage moduli and loss tangent of sample AB05C8.

Figure 22 shows the temperature dependence of the magnitude of the complex modulus,  $|E^*|$ , where  $|E^*| = \sqrt{(E')^2 + (E'')^2}$ , corresponding to the data shown in Figure 20. We find that the complex modulus is basically determined by the storage modulus, meaning that the contribution of viscous component in this temperature range for the viscoelastic properties of the composite polymer network is negligible.

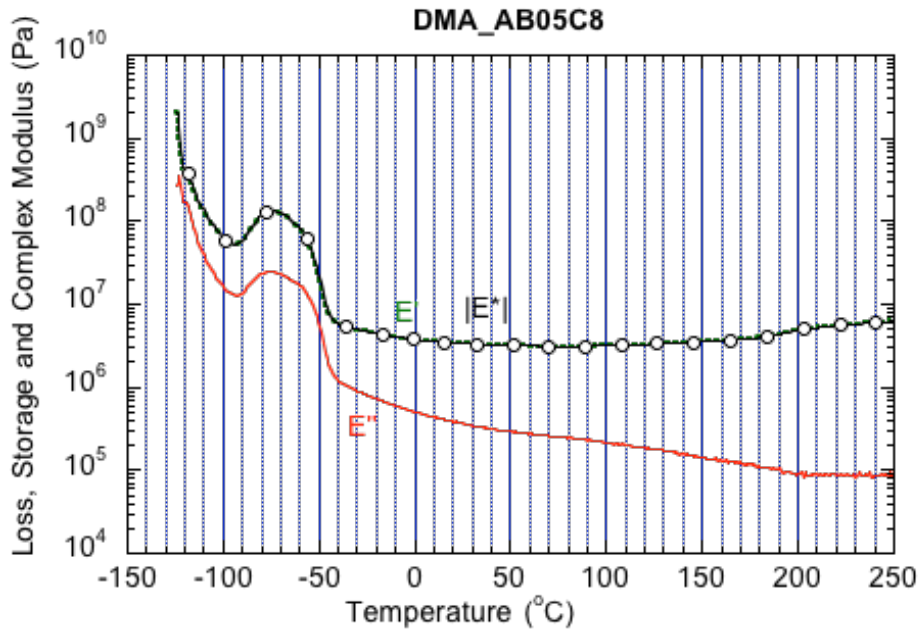


Figure 22: Comparison of the storage, loss and complex moduli of the sample AB05C8

Figure 23 shows a prototypical E-modulus master curve for a semicrystalline polymer network and which, we believe, provides a good description of our samples. Comparing with the figure 4, these samples are not showing the flow region due to the presence of cross-links, hence its polymer network nature

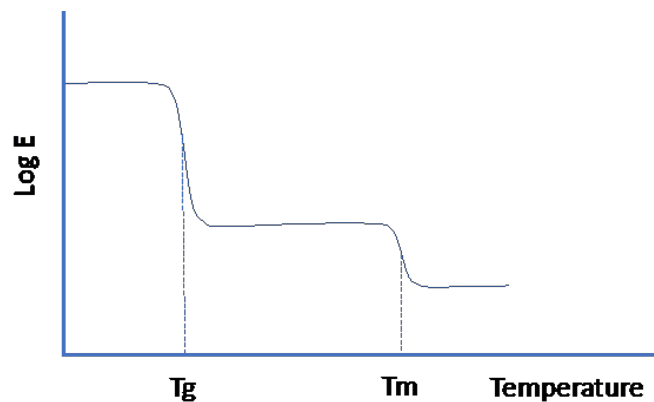


Figure 23: A schematic representation of the master curve E modulus-temperature that we propose for the PDMS/MWCNT nanocomposites. Three plateau regions are identified.

Figure 24-26 compare the effect of the MWCNT content on the samples' storage modulus for each cross-link content. We find a general trend of increased modulus with increased MWCNT content. However, there is not a monotonic increase for the three cross-link content samples. We believe that MWCNT aggregation and the consequent samples' composition heterogeneity are at origin of this behaviour. We note that the MWCNT were not chemically modified. Therefore, we expect that the interaction between the MWCNTs and the PDMS matrix is weak, leading to a small and non-monotonic effect.



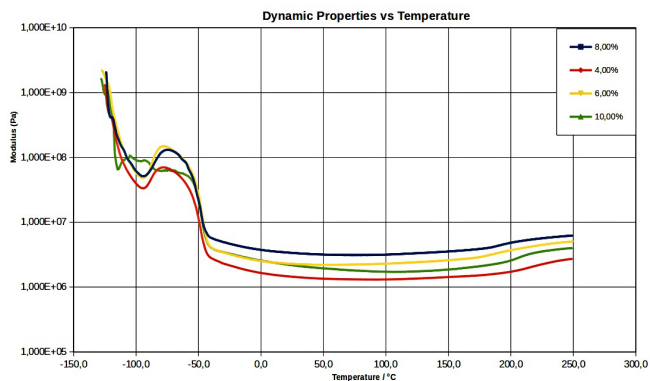


Figure 24: Variation of storage modulus with temperature for 5:1 cross-link density

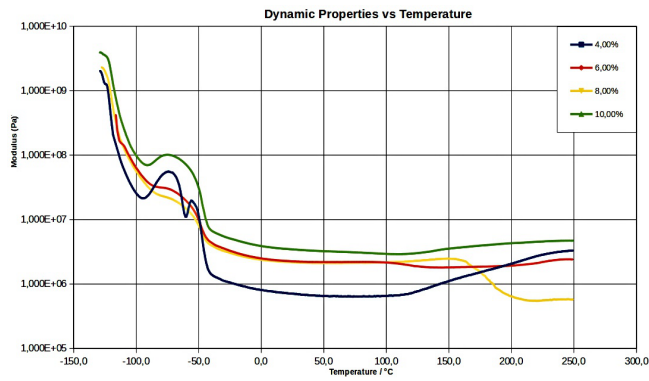


Figure 25: Variation of storage modulus with temperature for 10:1 Cross-link samples

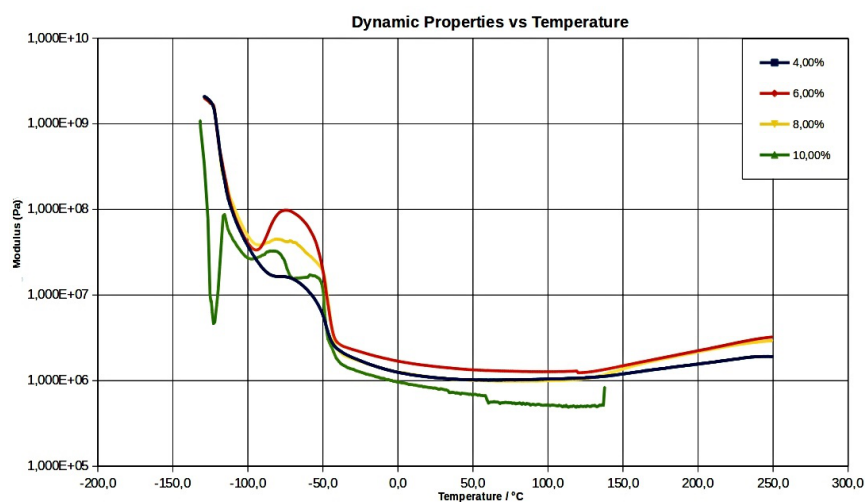
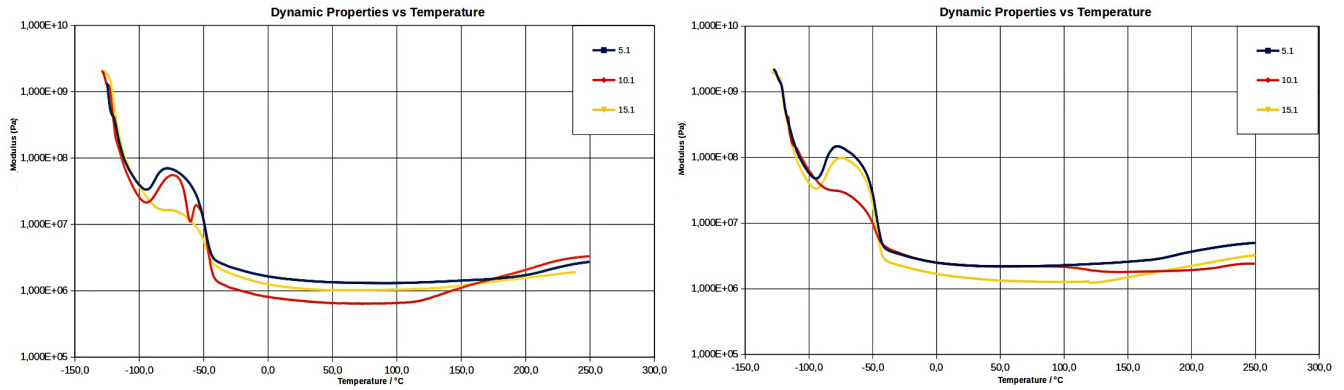
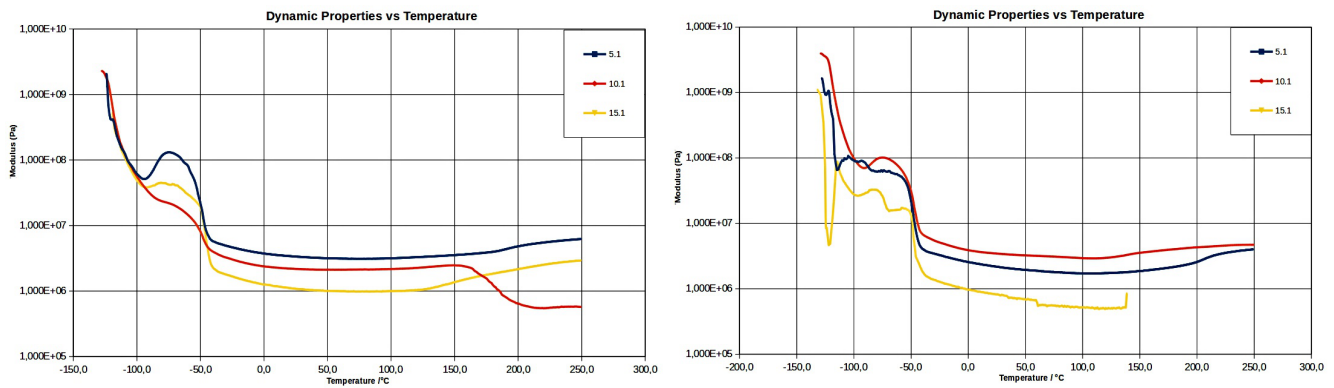


Figure 26: Variation of storage modulus with temperature for 15:1 Cross-link samples

Figure 27 shows the same information as that shown in Figure 24-26, but the data is organized in terms of the cross-link content for each MWCNT content. We would expect that an increase of Part A: Part B ratio, where Part B represents the cross-linking agent (see Table 1) should lead to a decrease of the storage modulus. That is the AB05 samples (possessing the highest cross-link content) should possess a higher storage modulus, while the AB15 samples should present the lower storage modulus. This prediction is not confirmed as shown in Figure 27. Again, we can only rationalise these results in terms of the samples heterogeneity.



(a) Storage modulus for 5:1, 10:1 and 15:1 with 4% Carbon Nanotube loading (b) Variation of storage modulus with temperature for 6% samples



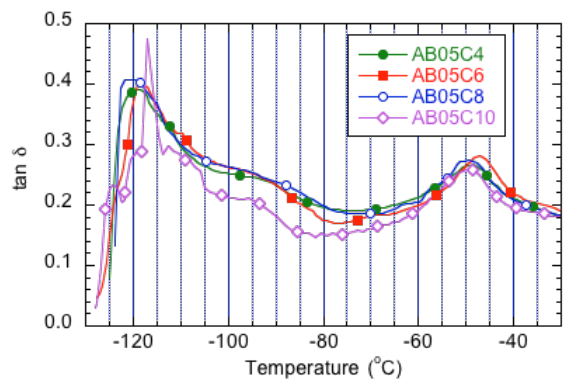
(c) Variation of storage modulus with temperature for 8% samples (d) Variation of storage modulus with temperature for 10% samples

Figure 27: Variation of the storage modulus of the PDMS/MWCNT nanocomposites as a function of the cross-link content for each MWCNT load.

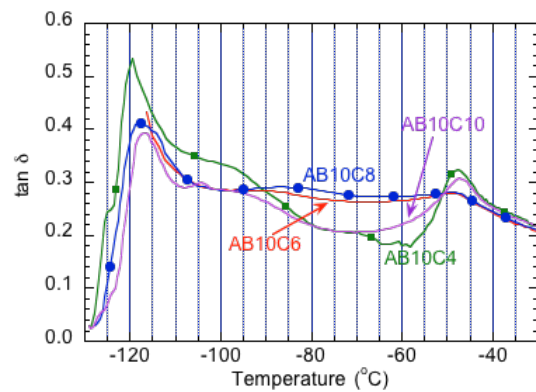
In addition to this somewhat erratic variation of the storage modulus with both the MWCNT load and the cross-link content, we found that above ca. 100°C an increase of the storage modulus occurs. As discussed above, this is a surprising result, for which we miss, at present, an explanation.

The addition of carbon nanotubes to a polymeric matrix can increase glass transition temperature due to interface interaction between carbon nanotube-polymers matrix [60]. This interaction decreases mobility of polymeric chains leading to an increase of its glass transition temperature.  $\tan \delta$  measures the energy dissipation of a material and translates how good it is absorbing energy. Upon applied stress close to the glass transition temperature, loss factor will increase due to the fact that polymeric chains have enough energy to move. The energy that is provided to the material by mechanic stimulus will be mostly absorbed (and lost) in form of polymeric chains movements (viscous behaviour). Therefore, at this temperature elastic properties (storage modulus) will decrease and viscous properties (loss factor) increase. As mentioned above, the temperature (at ca. -120°C) at which a maximum value for  $\tan \delta$  is observed can therefore be considered the glass transition temperature.

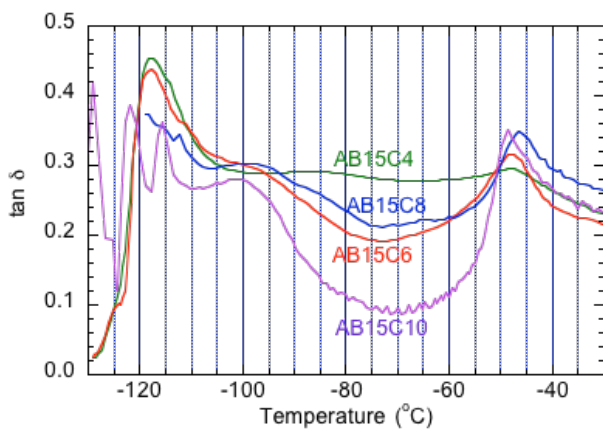
Figures 28 and 29 summarize the variation of  $\tan \delta$  with temperature for all samples. Analysing the position of the highest intensity peak, the one associated to the glass transition temperature, we conclude that is harder to establish a relationship between either the MWCNT content or the cross-link content. Table 2 summarizes the temperature at which this first peak of  $\tan \delta$  occurs, and which, tentatively is identified as the glass transition temperature. It is worth pointing out that that such Tg values are close to the starting temperature. Therefore, thermal stabilization effects may have a significant impact. Samples heterogeneity, as mentioned above, are likely a contributing factor for such spreading of values.



(a) 5:1

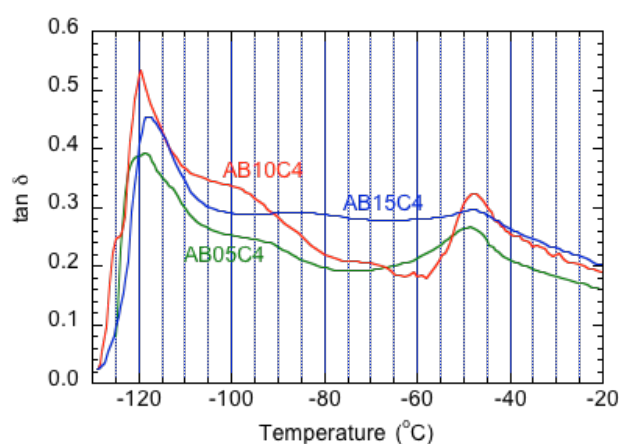


(b) 10:1

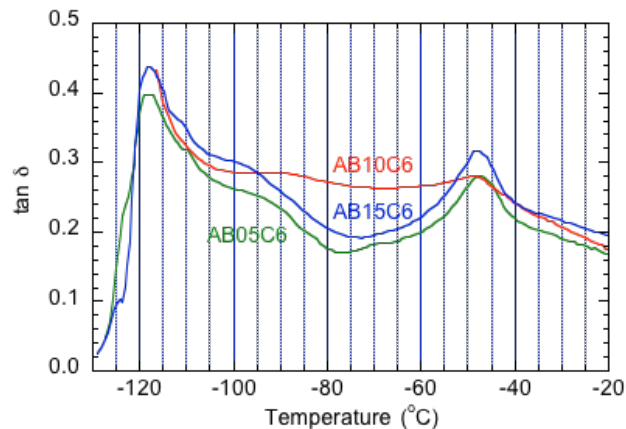


(c) 15:1

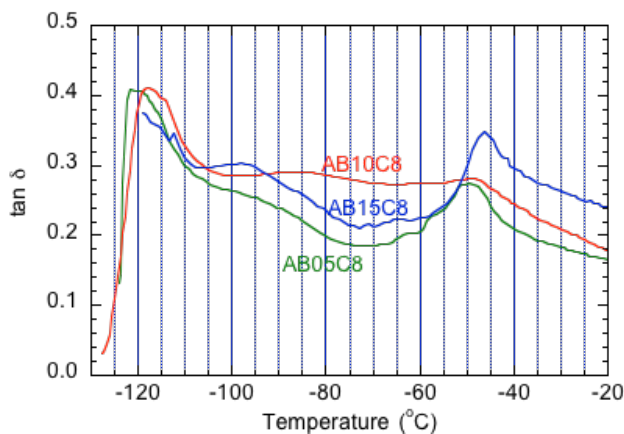
Figure 28: Variation of  $\tan\delta$  of the PDMS/MWCNT nanocomposites as a function of the MWCNT content for each cross-link content



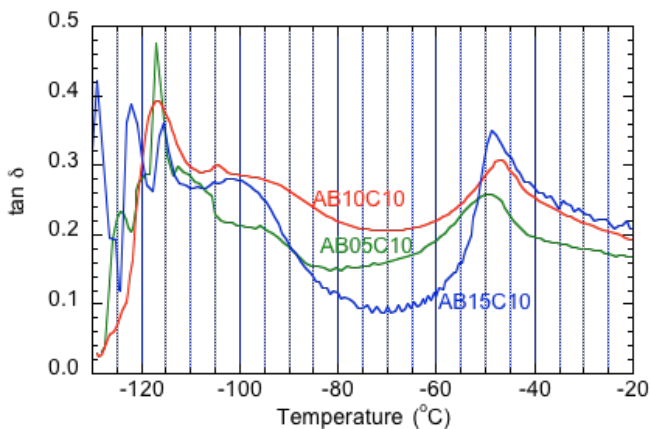
(a) 4%



(b) 6%



(c) 8%



(d) 10%

Figure 29: Variation of  $\tan \delta$  of the PDMS/MWCNT nanocomposites as a function of the cross-link content for each MWCNT load.

Table 2: Glass transition temperature ( $^{\circ}\text{C}$ ) of the twelve samples determined from the  $\tan \delta$  data.

Part A: Part B	MWCNT weight %			
	4%	6%	8%	10%
5:1	-118.7	-118.4	-121.6	-117
10:1	-117	< -116.3	-118.2	-116.5
15:1	-115.7	-117.8	< -119	-122

In conclusion, no direct correlation between the determined values of  $T_g$  and either the cross-link content or the MWCNT load is found.

The right-hand side peak of  $\tan \delta$  (Figures 28 and 29) is the one we associate to the melting of the crystalline domains. We could not identify a clear effect of either the MWCNT content or the cross-link content on the melting temperature  $T_m$ . Results are shown in Table 3. It should be mentioned that only minor effects would be expected and which would be related with, for instance, crystallite size. This spreading in the  $T_m$  values are, again, another signature of samples heterogeneity.

The melting temperatures of all samples are in the range -46.4 °C to -49.5 °C, which is a quite narrow range, as expected.

Table 3: Melting temperature (°C) of the twelve samples determined from the tan  $\delta$  data

Part A: Part B \ MWCNT weight %	4%	6%	8%	10%
5:1	-48.5	-47.2	-49.5	-48.7
10:1	-47.8	-49.5	-49.4	-47.3
15:1	-48.1	-48.1	-46.4	-48.7

In conclusion, both the mechanical properties (as assessed by DMA) and the glass transition temperature present some random dependence on both the cross-link content and the MWCNT load, being this randomness attributed to samples heterogeneity.

### 3.2 Electrical properties of PDMS/carbon nanotubes composites

The electrical properties of PDMS/carbon nanotubes composites were determined under static conditions (i.e. without dynamic or static samples deformation) using the four-contact method to assess the role of MWCNT content. A second study involved the evaluation of temperature effect. Finally, the variation of samples resistance upon mechanical deformation was studied using the two-point contact method. To further analyse if the electric properties of the composite are affected when cyclic tension and temperature variation is applied, electrical measurements were performed before and after Dynamic Mechanical Analysis.

#### 3.2.1 Electrical characterization

In order to investigate the effect of the MWCNT load on the electrical properties of the nanocomposites, we determined the electrical conductivity of the four samples containing a 10:1 cross-link content (samples AB10C4, AB10C6, AB10C8 and AB10C10) at room temperature. After the curing process, four gold electrodes, 250 nm thick, were deposited on the top of each sample (Figure 30) in order to reduce contact resistance, as shown in Scheme 1.



Figure 30: PDMS/carbon nanotube sample with two sets of deposited gold electrodes. Typical dimensions (width: 6 mm, thickness:1 mm, length: 2 cm).

Table 4: Conductivity (and resistivity) results of the measurements.

Sample	AB10C4	AB10C6	AB10C8	AB10C10
MWCNT content %	4%	6%	8%	10%
Thickness(mm)	0.3	0.3	0.6	1
Width(mm)	6	6	6	6
Length(mm)	0.3	0.3	0.3	0.3
$\rho$ (ohm.m)	11208	315	34.98	21.66
$\sigma$ (S/m)	$8.9 \times 10^{-5}$	$3.1 \times 10^{-3}$	$2.8 \times 10^{-2}$	$4.6 \times 10^{-2}$

To better visualize the effect of the MWCNT load, the conductivity results are represented in Figure 31.

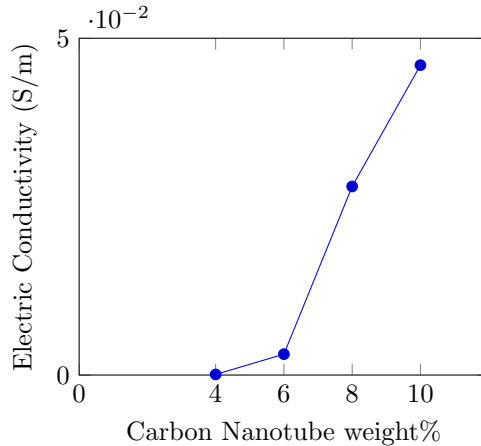


Figure 31: Electrical conductivity of the PDMS/MWCNT nanocomposites as a function of the MWCNT load at room temperature. The line is a guide to the eye.

PDMS matrix is electrically insulating. The electrical conductivity of the composites is due to the presence of the MWCNT. The carbon nanotubes used in these composites have diameters and length of 150-200nm and 5mm, respectively. The macroscopic charge transport of the samples depends on the ability of the electrons to hop between adjacent MWCNT in response to an external electrical field. Electron mobility in MWCNT is very large and it is this hopping process that limits the bulk conductivity. The hopping probability depends on the distance between MWCNT (and therefore on its concentration) and on the temperature (this being a thermally activated process)-percolation theory.

It should be mentioned that, while single-walled carbon nanotubes can exhibit metallic/semiconducting behaviour, there is a large probability that MWCNT will contain some metallic tubes, and are, therefore, preferred when we intend to obtain a conductive composite.

PDMS/MWCNT composites with 3% MWCT load were also prepared but we could not obtain a measurable resistance, and they were therefore discarded from this study.

Typically, the conductivity of composites combining an insulating matrix and a conductive filler shows an S-shape dependence on the filler load [61], pretty much resembling the results shown in Figure 31. At low load levels, there is a small increase of conductivity with the conductive filler content, which is attributed to an increased probability of inter-MWCNT electron hopping. This corresponds to the variation of the electrical conductivity when the MWCNT content increase from 4 to 6%. However, no continuous paths for the charges are significantly found. Then, after some critical content, which in the MWCNT fillers will depend on their length, there is sharp conductivity increase, meaning that a significant number of conductive paths are created. This sharp increase is observed when the MWCNT concentration increases from 6 up to 10%. Then, at higher concentrations, the conductivity shows a much weaker dependence on the filler concentration.

In the samples studied, we find a conductivity of only  $8.9 \times 10^{-5}$  S/m for the AB10C4 sample, which increases to  $4.6 \times 10^{-2}$  S/m for the AB10C10 sample. We anticipate that upon further increase of the MWCNT content the conductivity will further increase. However, for the aimed application, the conductivity achieve was considered adequate. In order to have high pressure-sensitive samples, the conductivity should be around the percolation threshold (see Figure 14). Furthermore, we suspected that samples with higher MWCNT content could show non ideal mechanical properties (namely a too high storage modulus). It turned out that, as shown in Figures 24-26, there is not a monotonic increase of the storage modulus with increased MWCNT content. We propose that the current study should be extended to samples with higher MWCNT content.



### 3.2.2 Effect of temperature on the electrical resistance

As mentioned above, according to the percolation theory, the electron transport in these composites will depend mainly on the distance between neighbouring MWCNTs, hence the strong dependence of the electrical conductivity of the composites on the MWCNT content. The hopping of the electrons between MWCNT is thermally activated, therefore we expect that the conductivity will increase with temperature. In addition, temperature increase may lead to an expansion of the matrix and may also influence the electron conductivity within each MWCNT. We consider that the electron transport within each MWCNT will not be significantly affected by the temperature, as we expect that the transport is determined by the presence of metallic carbon nanotubes within the MWCNT assembly, and their conductivity is not expected to be significantly sensitive to the temperature. However, if the transport is band-like, as in a metal, the temperature should promote a decrease in the conductivity.

We carried out a very simple study of the effect of temperature on the electrical resistance of two samples AB10C4 and AB10C8. The electrical conductivity at room temperature of these two samples was presented in the previous sections. As shown in Figure 31, sample AB10C4 is below the critical MWCNT concentration of 6%, at which the big conductivity increase starts, while the sample AB10C8 is in the transition range. We used a simple two-contact arrangement, to measure directly the resistance of the samples (which will include both the contacts and the sample resistance).

After the curing process, two silver electrodes were deposited on the surface of PDMS/Carbon Nanotubes samples using a silver paste. Figure 32 shows a picture of the setup used to increase sample's temperature and measure its resistance. The sample was placed on a heating plate to increase its temperature which was determined with a thermocouple. A digital multimeter was used to measure the electrical resistance at some temperature points, after thermal stabilization.



Figure 32: Picture of the setup for electrical resistance measurement with temperature variation.

Fig 33 shows the results obtained for 4% and 8% carbon nanotubes with cross-link content of 10:1. Surprisingly, the resistance increases with temperature.



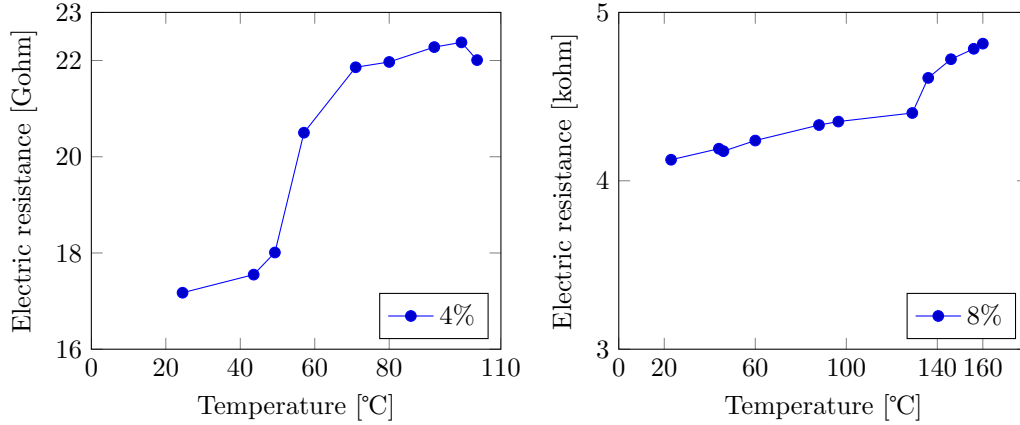


Figure 33: Effect of the temperature on the resistance of samples AB10C4 and AB10C8. The lines are guides to the eye.

As shown in Figure 33, when the temperature increases from 23°C to 100°C, an increment of electrical resistance of 30% and 5% is verified for 4% and 8% composites, respectively. Considering the factors that were discussed above that influence the electrical resistance of the composites and which depend, themselves, on the temperature, this increased resistance is attributed to an increased separation between the MWCNT, which, in turn, results from an expansion of the PDMS matrix. It is worth noting the stronger effect observed in the sample with lower MWCNT content, below the critical content required to reach significant percolation paths formation. The low concentration means that fewer close contacts between MWCNT (either between isolated MWCNT or between MWCNT bundles) exist, leading to a stronger effect of the expansion on the samples' resistance. We cannot disregard possible variation of the contact resistance with temperature, but this effect is harder to address.

### 3.2.3 Influence of the DMA studies on the electrical properties

Previous studies showed that polymeric composites under tension or compression may suffer reorientation of conductive fillers.[62][63]. In order to assess the effect of the DMA studies(cyclic stress/strain and temperature) on PDMS/carbon nanotubes electrical properties of the 12 samples, their electrical resistance was measured before and after Dynamic Thermal Mechanical Analysis, using the two-contact method, where the contacts were made with silver paste. From the resistance values, the electrical conductivity was calculated . The results are shown in Table 5.

Table 5: Electrical properties before and after Dynamic Mechanical Analysis.

CNT %	Cross-link	Conductivity(S/m)		Conductivity variation (%)
		Before	After	
4%	5:1	$11.73 \times 10^{-8}$	$83.33 \times 10^{-12}$	$-14.06 \times 10^3$
	10:1	$33.61 \times 10^{-10}$	$16.67 \times 10^{-9}$	101
	15:1	$89.28 \times 10^{-10}$	$0.05 \times 10^{-5}$	98
6%	5:1	$46.0 \times 10^{-5}$	$54.47 \times 10^{-6}$	-234,02
	10:1	$50.00 \times 10^{-7}$	$33.33 \times 10^{-9}$	$-14.90 \times 10^3$
	15:1	$60.00 \times 10^{-5}$	$75.75 \times 10^{-5}$	-26,21
8%	5:1	$28.476 \times 10^{-3}$	$22.73 \times 10^{-3}$	-25
	10:1	$21.07 \times 10^{-4}$	$18.522 \times 10^{-3}$	-88,62
	15:1	$21.00 \times 10^{-3}$	$26.59 \times 10^{-4}$	$-68.96 \times 10^1$
10%	5:1	$77.16 \times 10^{-3}$	$37.20 \times 10^{-5}$	$-20.64 \times 10^3$
	10:1	$12.77 \times 10^{-3}$	$37.20 \times 10^{-5}$	$-33.32 \times 10^2$
	15:1	$11.00 \times 10^{-2}$	$45.79 \times 10^{-5}$	$-24.17 \times 10^3$

Table 5 shows that there is not a consistent effect of the mechanical and thermal stress impinged on the samples during the DMA investigations on the samples' conductivity. The magnitude of the variation is also very broad. All samples with 6, 8 or 10% MWCNT content undergo a reduction of conductivity, while the samples with 4% show a mixed effect. It is not possible either to conclude about the effect of the cross-link content on the conductivity variation. This observation is likely related to the absence of clear correlation between the Part A:Part B ratio of the samples and the corresponding mechanical properties (as discussed above). Despite the systematic study, we could not relate sample composition with mechanical properties and this impacts also on the absence of a correlation with the electrical stability upon DMA analysis. Carbon nanotubes have a strong tendency to aggregate, forming bundles, due to the strong van der Waals interactions between them. It is reasonable to assume that the dynamic mechanical stress and the temperature cycling could facilitate their aggregation, reducing the percolation and leading to a decreased conductivity. This would be the most likely anticipated result. Though observed for most samples, this is not observed for all samples. We should also mention that, being the electrical conductivity determined by the two-contacts method, a possible degradation of their interaction with the surface of the sample, thereby increasing the contact resistance, is also a contributor to the decrease of the calculated samples conductivity.

### 3.2.4 Sensing effect of applied stress on materials resistance

The purpose of this project consists on the development and characterization of a nanocomposite to be used as a pressure sensor. For that, is important to analyse the variation of electrical properties upon application of a mechanical stimulus. Samples with 4, 6, 8 and 10% with 10:1 cross-link content (samples AB10) were studied. A strain of 50% (elongation) was applied and the achieved resistance was compared to the initial (undeformed sample) value. Table 6 summarizes the obtained results, which evidence a huge resistance variation upon deformation.

Table 6: Variation of the electrical resistance of AB10 samples upon an elongation strain of 50%

CNT%	Electric Resistance Variation(%)
4%	2677.77
6%	1886.31
8%	1100.52
10%	1265.22

From table 6, it is possible to notice that the variation of electrical resistance upon deformation is lower for higher carbon nanotubes loadings.

For higher CNT loadings in a polymeric matrix, the number of contacts between carbon nanotubes increases and so does the electrical conductivity. Upon stretching of the material, contacts between carbon nanotubes are broken and the conductive network is destabilized. Due to the higher density of contacts between carbon nanotubes existing on 10% CNT samples, the impact of 50% deformation on electrical properties is less pronounced for higher higher carbon nanotubes loadings. Despite the general decrease of the relative resistance variation upon increase of the MWCNT content, we find that such decrease is slightly lower for the sample with 8% than that of the sample with 10% MWCNT. This result is difficult to explain if we assume that we have samples with homogeneous distribution of the MWCNT and without variation of the contact resistance during the deformation. These two assumptions are probably (and most likely) not entirely valid, which may explain the result.

## 4 Conclusions

In this study, 12 PDMS/MWCNT samples were studied in order to evaluate the effects of cross-link and CNT % variation on the mechanical, thermal and electrical properties. Some challenges needed to be addressed before the preparation of the sample, namely the dispersion of MWCNT on the pristine PDMS. Several dispersion times were studied in order to achieve a good dispersion of th MWCNT in the solvent, for the different MWCNT concentrations. Also, due to the viscosity of PDMS, air bubbles were easily trapped inside PDMS/MWCNT samples, that would expand upon polymerization in the furnace and affect its conductive and mechanical behavior. To mitigate the problem, the samples were placed in a vacuum chamber at room temperature for 1h before polymerization in order to reduce the number of bubbles as much as possible. In general, DMA studies demonstrated increase of the modulus with the MWCNT content for a fixed cross-link density ( Figures 24-26) , but no monotonic increase was observed for the three cross-link samples( Figure 27). This observation can be explained by possible non homogeneity of the samples. The value of the glass transition temperature was also assessed but no correlation between T<sub>g</sub>, cross-link density and CN content was observed, as shown in table 2. This result can also be explained by possible non homogeneity of the samples and poor thermal stabilization. It was observed that for higher values of CN content, the electrical conductivity also increases, which was expected. As shown in Figure 31, from 4% to 6% the electrical conductivity does not increase as much as from 6% to 8%. This can be explained by the number of MWCNT contacts/paths that are created. After a critical CNT % value, it is observed a sharp increase in the conductivity which can be explained the significant number of conductive paths that are created. Higher CNT concentration was not studied but we anticipate that upon further increase of the MWCNT content, the conductivity will increase. The effect of temperature variation on electrical resistance was also studied ( Figure 33) for AB10C4 and AB10C8. Upon temperature rise, AB10C8 showed more stability, less electric resistance variation, than AB10C4. Samples with lower MWCNT % has less contacts between MWCNT, therefore, a stronger effect of PDMS matrix is observed on sample's resistance.

The electrical conductivity before and after DMA studies was performed (Table 5), however it is not possible to address a conclusion due to inconsistent effect of the mechanical and thermal stress on electrical conductivity.

The variation of electrical resistance was determined upon applied 50% sample elongation (Table 6). In general, it was observed that when MWCNT % increase, the sample is less prone to electrical resistance variation upon elongation. AB10C10 showed more electrical resistance variation than AB10C8. This result can be explained by possible non homogeneity of the sample.

As explained before, the fact that some results did not go according to what was expected may be due to non homogeneity of the solutions. From the experiment it was noticeable(visually) the increase in viscosity of the samples when MWCNT content increased from 6% to 10%. Therefore, the dispersion of 10% MWCNT in PDMS need to be adjusted in order to achieve a better sample homogeneity. Some MWCNT agglomeration was observed for 10% MWCNT samples. Not only the dispersion but the preparation of the samples with more MWCNT and cross-link was challenging. Sample AB15C10 was synthesised several times because after polymerization it was brittle and fragile. It was observed (visually) that samples with more MWCNT % content and less cross-link density (AB15C10, AB15C8) were more difficult to obtain as thin films.

In view of the huge resistance variation upon deformation of the PDMS/MWCNT nanocomposites, which indicates that this is indeed a system that is well-suited for a pressure sensor, we believe that further effort should be devoted to the preparation and characterization of new samples, and obtain a more consistent description of their properties.

## 5 Institutes

The development of this project involved both CeNTI (Center of Nanotechnology and Technical, Functional and Smart Materials) located in Vila Nova de Famalicão and the Organic Electronics Group of Instituto de Telecomunicações-Lisbon. CeNTI is a non-profit private Institute that develops Research activities, Technological development, Innovation and Engineering in materials and also in functional and smart systems. CeNTI was founded in 2006 and it is the result of a partnership with 3 Universities, 2 Technological Centers and 1 New Technological Institute, all recognized by their national and international relevance: Minho University, Porto University, Aveiro University, CITEVE-Technological Center of Textil Industry and Clothing of Portugal, CTIC-Technological Center of Leather Industry and CEIIA-Centre for Excellence and Innovation in Automobile Industry. CeNTI activities encompass various fields such as Polymers and Functional Coatings, Functional Fibers, Functional Nanomaterials and also Smart Systems and Materials.



CeNTI

Instituto de Telecomunicações (IT) is a private, non-profit, association of six Portuguese universities, one polytechnic, one public telecom operator and one telecom equipment manufacturer, established in 1992 with a mission to create and share scientific knowledge in telecommunications at world level and to host and tutor graduate and post-graduate students. IT earned the statute of Associated Laboratory in 2001. IT is organized around three main sites: Aveiro, Coimbra and Lisbon with delegations in Covilha, Leiria, Lisbon and Porto. IT hosts more than 300 (PhD holding) researchers, 7 of which are Fellows of IEEE, and 3 Fellows of the IET, 200 PhD Students and 200 MSc students. IT expertise spans all areas of telecommunications and supporting sciences including wireless and optical communications, networks and multimedia. The Organic Electronics Group (oeG) at IT has a broad activity area, encompassing the synthesis, characterization and application in electronics, optoelectronics and bioelectronics of organic conductors and semiconductors.



IT

## References

- [1] I D Johnston, D K McCluskey, C K L Tan, and M C Tracey. Mechanical characterization of bulk sylgard 184 for microfluidics and microengineering. *Journal of Micromechanics and Microengineering*, 24(3):035017, February 2014.
- [2] Saleem Khan, L. Lorenzelli, and R. S. Dahiya. Bendable piezoresistive sensors by screen printing MW-CNT/PDMS composites on flexible substrates. In *2014 10th Conference on Ph.D. Research in Microelectronics and Electronics (PRIME)*. IEEE, June 2014.
- [3] Jeong Hun Kim, Ji-Young Hwang, Ha Ryeon Hwang, Han Seop Kim, Joong Hoon Lee, Jae-Won Seo, Ueon Sang Shin, and Sang-Hoon Lee. Simple and cost-effective method of highly conductive and elastic carbon nanotube/polydimethylsiloxane composite for wearable electronics. *Scientific Reports*, 8(1), January 2018.
- [4] Alamusi, Ning Hu, Hisao Fukunaga, Satoshi Atobe, Yaolu Liu, and Jinhua Li. Piezoresistive strain sensors made from carbon nanotubes based polymer nanocomposites. *Sensors*, 11(11):10691–10723, November 2011.
- [5] Peng-Cheng Ma, Naveed A. Siddiqui, Gad Marom, and Jang-Kyo Kim. Dispersion and functionalization of carbon nanotubes for polymer-based nanocomposites: A review. *Composites Part A: Applied Science and Manufacturing*, 41(10):1345–1367, October 2010.
- [6] J. Yun, C. Rago, I. Cheong, R. Pagliarini, P. Angenendt, H. Rajagopalan, K. Schmidt, J. K. V. Willson, S. Markowitz, S. Zhou, L. A. Diaz, V. E. Velculescu, C. Lengauer, K. W. Kinzler, B. Vogelstein, and N. Papadopoulos. Glucose deprivation contributes to the development of KRAS pathway mutations in tumor cells. *Science*, 325(5947):1555–1559, August 2009.
- [7] Jacob Fraden. *Handbook of Modern Sensors*. Springer International Publishing, 2016.
- [8] Ahmed M. Almassri, W. Z. Wan Hasan, S. A. Ahmad, A. J. Ishak, A. M. Ghazali, D. N. Talib, and Chikamune Wada. Pressure sensor: State of the art, design, and application for robotic hand. *Journal of Sensors*, 2015:1–12, 2015.
- [9] Vasileios Mitrakos, Lisa Macintyre, Fiona Denison, Philip Hands, and Marc Desmulliez. Design, manufacture and testing of capacitive pressure sensors for low-pressure measurement ranges. *Micromachines*, 8(2):41, February 2017.
- [10] Rajarajan Ramalingame, Amoog Lakshmanan, Florian Müller, Ulrike Thomas, and Olfa Kanoun. Highly sensitive capacitive pressure sensors for robotic applications based on carbon nanotubes and PDMS polymer nanocomposite. *Journal of Sensors and Sensor Systems*, 8(1):87–94, February 2019.
- [11] A.A. Barlian, W.-T. Park, J.R. Mallon, A.J. Rastegar, and B.L. Pruitt. Review: Semiconductor piezoresistance for microsystems. *Proceedings of the IEEE*, 97(3):513–552, March 2009.
- [12] Sarang S. Bari, Aniruddha Chatterjee, and Satyendra Mishra. Biodegradable polymer nanocomposites: An overview. *Polymer Reviews*, 56(2):287–328, January 2016.
- [13] Robert J. Young. *Introduction to Polymers*. Springer, jan 1983.
- [14] Ferdinand Rodriguez. *Principles of Polymer Systems*. CRC Press, dec 2014.
- [15] L.H. Sperling. *Introduction to Physical Polymer Science*. John Wiley & Sons, Inc., November 2005.
- [16] Lanhua Wei, P. K. Kuo, R. L. Thomas, T. R. Anthony, and W. F. Banholzer. Thermal conductivity of isotopically modified single crystal diamond. *Physical Review Letters*, 70(24):3764–3767, June 1993.
- [17] L. Gołuński, K. Zwolski, and P. Płotka. Electrical characterization of diamond/boron doped diamond nanostructures for use in harsh environment applications. *IOP Conference Series: Materials Science and Engineering*, 104:012022, January 2016.

- [18] R Saito, G Dresselhaus, and M S Dresselhaus. *Physical Properties of Carbon Nanotubes*. PUBLISHED BY IMPERIAL COLLEGE PRESS AND DISTRIBUTED BY WORLD SCIENTIFIC PUBLISHING CO., July 1998.
- [19] Sumio Iijima. Helical microtubules of graphitic carbon. *Nature*, 354(6348):56–58, November 1991.
- [20] Cuong Duong-Viet, Housseinou Ba, Lai Truong-Phuoc, Yuefeng Liu, Jean-Philippe Tessonnier, Jean-Mario Nhut, Pascal Granger, and Cuong Pham-Huu. Nitrogen-doped carbon composites as metal-free catalysts. In *New Materials for Catalytic Applications*, pages 273–311. Elsevier, 2016.
- [21] T. W. Ebbesen, H. J. Lezec, H. Hiura, J. W. Bennett, H. F. Ghaemi, and T. Thio. Electrical conductivity of individual carbon nanotubes. *Nature*, 382(6586):54–56, July 1996.
- [22] Antonio Maffucci, Sergey A. Maksimenko, Giovanni Miano, and Gregory Ya. Slepyan. Electrical conductivity of carbon nanotubes: Modeling and characterization. In *Carbon Nanotubes for Interconnects*, pages 101–128. Springer International Publishing, July 2016.
- [23] P.G. Collins and Ph. Avouris. Multishell conduction in multiwalled carbon nanotubes. *Applied Physics A: Materials Science & Processing*, 74(3):329–332, March 2002.
- [24] Meysam Rahmat and Pascal Hubert. Carbon nanotube–polymer interactions in nanocomposites: A review. *Composites Science and Technology*, 72(1):72–84, December 2011.
- [25] Vinay Deep Punetha, Sravendra Rana, Hye Jin Yoo, Alok Chaurasia, James T. McLeskey, Madeshwaran Sekkarapatti Ramasamy, Nanda Gopal Sahoo, and Jae Whan Cho. Functionalization of carbon nanomaterials for advanced polymer nanocomposites: A comparison study between CNT and graphene. *Progress in Polymer Science*, 67:1–47, April 2017.
- [26] Alvaro Mata, Aaron J. Fleischman, and Shuvo Roy. Characterization of polydimethylsiloxane (PDMS) properties for biomedical micro/nanosystems. *Biomedical Microdevices*, 7(4):281–293, December 2005.
- [27] Eileen Pedraza, Ann-Christina Brady, Christopher A. Fraker, and Cherie L. Stabler. Synthesis of macroporous poly(dimethylsiloxane) scaffolds for tissue engineering applications. *Journal of Biomaterials Science, Polymer Edition*, 24(9):1041–1056, October 2012.
- [28] Rachelle N. Palchesko, Ling Zhang, Yan Sun, and Adam W. Feinberg. Development of polydimethylsiloxane substrates with tunable elastic modulus to study cell mechanobiology in muscle and nerve. *PLoS ONE*, 7(12):e51499, December 2012.
- [29] Baolin Zhang, Ping Zhang, Hanzhi Zhang, Casey Yan, Zijian Zheng, Biao Wu, and You Yu. A transparent, highly stretchable, autonomous self-healing poly(dimethyl siloxane) elastomer. *Macromolecular Rapid Communications*, 38(15):1700110, May 2017.
- [30] D. Qian, E. C. Dickey, R. Andrews, and T. Rantell. Load transfer and deformation mechanisms in carbon nanotube-polystyrene composites. *Applied Physics Letters*, 76(20):2868–2870, May 2000.
- [31] M. J. Biercuk, M. C. Llaguno, M. Radosavljevic, J. K. Hyun, A. T. Johnson, and J. E. Fischer. Carbon nanotube composites for thermal management. *Applied Physics Letters*, 80(15):2767–2769, April 2002.
- [32] M. Cadek, J. N. Coleman, V. Barron, K. Hedicke, and W. J. Blau. Morphological and mechanical properties of carbon-nanotube-reinforced semicrystalline and amorphous polymer composites. *Applied Physics Letters*, 81(27):5123–5125, December 2002.
- [33] Carlos Velasco-Santos, Ana L. Martínez-Hernández, Frank T. Fisher, Rodney Ruoff, and Victor M. Castaño. Improvement of thermal and mechanical properties of carbon nanotube composites through chemical functionalization. *Chemistry of Materials*, 15(23):4470–4475, November 2003.
- [34] J. Engel, J. Chen, Nannan Chen, S. Pandya, and Chang Liu. Multi-walled carbon nanotube filled conductive elastomers: Materials and application to micro transducers. In *19th IEEE International Conference on Micro Electro Mechanical Systems*. IEEE, 2006.

- [35] Chung-Lin Wu, Hsueh-Chu Lin, Chien-Hsin Huang, Ming-Chuen Yip, and Weileun Fang. Mechanical properties of PDMS/CNTs nanocomposites. *MRS Proceedings*, 1056, 2007.
- [36] Caroline McClory, Tony McNally, Mark Baxendale, Petra Pötschke, Werner Blau, and Manuel Ruether. Electrical and rheological percolation of PMMA/MWCNT nanocomposites as a function of CNT geometry and functionality. *European Polymer Journal*, 46(5):854–868, May 2010.
- [37] N. F. A. Zainal, A. A. Azira, S. F. Nik, M. Rusop, Mohamad Rusop, and Tetsuo Soga. The electrical and optical properties of PMMAMWCNTs nanocomposite thin films. In *AIP Conference Proceedings*. AIP, 2009.
- [38] E Kymakis, I Alexandou, and G.A.J Amaratunga. Single-walled carbon nanotube–polymer composites: electrical, optical and structural investigation. *Synthetic Metals*, 127(1-3):59–62, March 2002.
- [39] Chunying Min, Xiangqian Shen, Zhou Shi, Lei Chen, and Zhiwei Xu. The electrical properties and conducting mechanisms of carbon nanotube/polymer nanocomposites: A review. *Polymer-Plastics Technology and Engineering*, 49(12):1172–1181, September 2010.
- [40] J Sandler, M.S.P Shaffer, T Prasse, W Bauhofer, K Schulte, and A.H Windle. Development of a dispersion process for carbon nanotubes in an epoxy matrix and the resulting electrical properties. *Polymer*, 40(21):5967–5971, October 1999.
- [41] J.K.W. Sandler, J.E. Kirk, I.A. Kinloch, M.S.P. Shaffer, and A.H. Windle. Ultra-low electrical percolation threshold in carbon-nanotube-epoxy composites. *Polymer*, 44(19):5893–5899, September 2003.
- [42] Guangjun Hu, Chungui Zhao, Shimin Zhang, Mingshu Yang, and Zhigang Wang. Low percolation thresholds of electrical conductivity and rheology in poly(ethylene terephthalate) through the networks of multi-walled carbon nanotubes. *Polymer*, 47(1):480–488, January 2006.
- [43] Emmanuel Kymakis and Gehan A. J. Amaratunga. Electrical properties of single-wall carbon nanotube-polymer composite films. *Journal of Applied Physics*, 99(8):084302, April 2006.
- [44] J. O. Aguilar, J. R. Bautista-Quijano, and F. Aviles. Influence of carbon nanotube clustering on the electrical conductivity of polymer composite films. *Express Polymer Letters*, 4(5):292–299, 2010.
- [45] Zhi-Min Dang, Jun-Wei Zha, Khurram Shehzad, and Jing Zhang. Mechanism and properties of piezoresistive in rubber-matrix nanocomposites. In *Proceedings of 2011 International Symposium on Electrical Insulating Materials*. IEEE, September 2011.
- [46] M. Mohiuddin and S.V. Hoa. Temperature dependent electrical conductivity of CNT–PEEK composites. *Composites Science and Technology*, 72(1):21–27, December 2011.
- [47] M Norkhairunnisa, A Azizan, M Mariatti, H Ismail, and LC Sim. Thermal stability and electrical behavior of polydimethylsiloxane nanocomposites with carbon nanotubes and carbon black fillers. *Journal of Composite Materials*, 46(8):903–910, September 2011.
- [48] W.A. Khan W.S. Khan, N.N. Hamadneh. *Science and applications of Tailored Nanostructures*. One Central Press (OCP), University of Padova, Italy, 2016.
- [49] Niranjana Karak. Fundamentals of nanomaterials and polymer nanocomposites. In *Nanomaterials and Polymer Nanocomposites*, pages 1–45. Elsevier, 2019.
- [50] Chao-Xuan Liu and Jin-Woo Choi. Improved dispersion of carbon nanotubes in polymers at high concentrations. *Nanomaterials*, 2(4):329–347, October 2012.
- [51] GUOXING SUN, ZHENGPING LIU, and GUANGMING CHEN. DISPERSION OF PRISTINE MULTI-WALLED CARBON NANOTUBES IN COMMON ORGANIC SOLVENTS. *Nano*, 05(02):103–109, April 2010.
- [52] Low Foo Wah, Wei Wen Liu, U. Hashim, and Chin Wei Lai. The effect of chemical solutions (isopropyl alcohol, dichloromethane, acetone and triton x-100) on the dispersion of single-walled carbon nanotubes. *Advanced Materials Research*, 1109:113–117, June 2015.



- [53] Rajarajan Ramalingame, Pritha Chandraker, and Olfa Kanoun. Investigation on the influence of solvents on MWCNT-PDMS nanocomposite pressure sensitive films. *Proceedings*, 1(4):384, August 2017.
- [54] Nicola Bowler. Four-point potential drop measurements for materials characterization. *Measurement Science and Technology*, 22(1):012001, November 2010.
- [55] Kevin P. Menard and Noah R. Menard. Dynamic mechanical analysis in the analysis of polymers and rubbers, September 2015.
- [56] Shiuh-Chuan Her and Kuan-Yu Lin. Dynamic mechanical analysis of carbon nanotube-reinforced nanocomposites. *Journal of Applied Biomaterials & Functional Materials*, 15(Suppl. 1):0–0, 2017.
- [57] I. Perepechk. *Acoustic Methods of Investigating Polymers*. Mir Publishes, Moscow, 1975.
- [58] Dow Corning. *Product Information Silicon Elastomer Sylgard*, 2017.
- [59] T Dollase, H. W Spiess, M Gottlieb, and R Yerushalmi-Rozen. Crystallization of PDMS: The effect of physical and chemical crosslinks. *Europhysics Letters (EPL)*, 60(3):390–396, November 2002.
- [60] Yasin Kanbur and Umit Tayfun. Investigating mechanical, thermal, and flammability properties of thermoplastic polyurethane/carbon nanotube composites. *Journal of Thermoplastic Composite Materials*, 31(12):1661–1675, November 2017.
- [61] You Zeng, Guixia Lu, Han Wang, Jinhong Du, Zhe Ying, and Chang Liu. Positive temperature coefficient thermistors based on carbon nanotube/polymer composites. *Scientific Reports*, 4(1), October 2014.
- [62] J.R. Wood, Q. Zhao, and H.D. Wagner. Orientation of carbon nanotubes in polymers and its detection by raman spectroscopy. *Composites Part A: Applied Science and Manufacturing*, 32(3-4):391–399, March 2001.
- [63] Michael J. Lance, Chun-Hway Hsueh, Ilia N. Ivanov, and David B. Geohegan. Reorientation of carbon nanotubes in polymer matrix composites using compressive loading. *Journal of Materials Research*, 20(4):1026–1032, April 2005.